Late Quaternary deposition and facies model for karstic Lake Estanya (North-eastern Spain)

Morellón, Mario; Valero-Garcés, Blas; Anselmetti, Flavio S.; Ariztegui, Daniel; Schnellmann, Michael; Moreno, Ana; Mata, Pilar; Rico, Mayte; Corella, Juan Pablo

How to cite

MORELLÓN, Mario et al. Late Quaternary deposition and facies model for karstic Lake Estanya (North-eastern Spain). In: Sedimentology, 2009, vol. 56, n° 5, p. 1505–1534. doi: 10.1111/j.1365-3091.2008.01044.x

This publication URL: https://archive-ouverte.unige.ch/unige:17090

Publication DOI: 10.1111/j.1365-3091.2008.01044.x

SEDIMENTOLOGY the journal of the International Association of Sedimentologists

Sedimentology (2009) **56,** 1505–1534 doi: 10.1111/j.1365-3091.2008.01044.x

Late Quaternary deposition and facies model for karstic Lake Estanya (North-eastern Spain)

MARIO MORELLÓN*, BLAS VALERO-GARCÉS*, FLAVIO ANSELMETTI†, DANIEL ARIZTEGUI‡, MICHAEL SCHNELLMANN§, ANA MORENO*¶, PILAR MATA**, MAYTE RICO* and JUAN PABLO CORELLA*

**Department of Environmental Processes and Global Change, Pyrenean Institute of Ecology (IPE) – CSIC, Campus de Aula Dei, Avda Montañana 1005, E-50059 Zaragoza, Spain (E-mail: mariomm@ipe.csic.es)*

†EAWAG, Swiss Federal Institute of Aquatic Research, Ueberlandstrasse 133, CH-8600 Duebendorf, Switzerland

‡Section of Earth Sciences, University of Geneva, Rue des Maraîchers 13. CH-1205 Genève, Switzerland

§Geological Institute – Swiss Federal Institute of Technology, Zürich (ETH), Sonneggstrasse 5, CH-8092 Zürich, Switzerland

¶Limnological Research Center (LRC), Department of Geology and Geophysics, University of Minnesota, 220 Pillsbury Hall/310 Pillsbury Drive S.E., Minneapolis, MN 55455-0219, USA

***Facultad de Ciencias del Mar y Ambientales, Universidad de Cádiz, Polígono Río San Pedro s/n, 11510 Puerto Real (Cádiz), Spain*

Associate Editor: Stephen Lokier

ABSTRACT

Lake Estanya is a small (19 ha), freshwater to brackish, monomictic lake formed by the coalescence of two karstic sinkholes with maximum water depths of 12 and 20 m, located in the Pre-Pyrenean Ranges (North-eastern Spain). The lake is hydrologically closed and the water balance is controlled mostly by groundwater input and evaporation. Three main modern depositional sub-environments can be recognized as: (i) a carbonate-producing 'littoral platform'; (ii) a steep 'talus' dominated by reworking of littoral sediments and mass-wasting processes; and (iii) an 'offshore, distal area', seasonally affected by anoxia with fine-grained, clastic sediment deposition. A seismic survey identified up to 15 m thick sedimentary infill comprising: (i) a 'basal unit', seismically transparent and restricted to the depocentres of both sub-basins; (ii) an 'intermediate unit' characterized by continuous high-amplitude reflections; and (iii) an 'upper unit' with strong parallel reflectors. Several mass-wasting deposits occur in both sub-basins. Five sediment cores were analysed using sedimentological, microscopic, geochemical and physical techniques. The chronological model for the sediment sequence is based on 17 accelerator mass spectrometry ^{14}C dates. Five depositional environments were characterized by their respective sedimentary facies associations. The depositional history of Lake Estanya during the last *ca* 21 kyr comprises five stages: (i) a brackish, shallow, calcite-producing lake during full glacial times (21 to 17·3 kyr BP); (ii) a saline, permanent, relatively deep lake during the late glacial (17·3 to 11·6 kyr BP); (iii) an ephemeral, saline lake and saline mudflat complex during the transition to the Holocene (11·6 to 9·4 kyr BP); (iv) a saline lake with gypsum-rich, laminated facies and abundant microbial mats punctuated by periods of more frequent flooding episodes and clastic-dominated deposition during the Holocene (9·4 to 0·8 kyr BP); and (v) a deep, freshwater to brackish lake with high clastic input during the last 800 years. Climate-driven hydrological fluctuations are the main internal control in the evolution of the lake during the last 21 kyr,

affecting water salinity, lake-level changes and water stratification. However, external factors, such as karstic processes, clastic input and the occurrence of mass-flows, are also significant. The facies model defined for Lake Estanya is an essential tool for deciphering the main factors influencing lake deposition and to evaluate the most suitable proxies for lake level, climate and environmental reconstructions, and it is applicable to modern karstic lakes and to ancient lacustrine formations.

Keywords Iberian Peninsula, karstic lake, lacustrine depositional environments, Late Quaternary, mass flow, palaeohydrology, sedimentary facies, seismic stratigraphy.

INTRODUCTION

Quaternary lacustrine systems have been studied extensively in the last decades (Gierlowski-Kordesch & Kelts, 1994, 2000; Cohen, 2003). New depositional models have been described for a number of lake types based on modern systems and Quaternary basins: playa, ephemeral and shallow saline lakes (Eugster & Hardie, 1978; Hardie *et al.*, 1978; Eugster & Kelts, 1983; Last, 1990; Smoot & Lowenstein, 1991; Renault & Last, 1994; Schreiber & Tabakh, 2000), carbonate-rich lakes (Platt & Wright, 1991), volcanic-related lakes (Negendank & Zolitschka, 1993; Nelson *et al.*, 1994), tectonic basins (Lambiase, 1990), glacial (Jopling, 1975) and fluvial lakes (Bohacks *et al.*, 2000). Several projects coordinated by the International Continental Scientific Deep Drilling Project have provided new seismic and core data for large and deep lake basins [for example, Great Salt Lake (Balch *et al.*, 2005); Titicaca, (Fritz *et al.*, 2007); Malawi, (Brown *et al.*, 2007); and Petzen Itza (Anselmetti *et al.*, 2006; Hodell *et al.*, 2008)].

Considerably less attention has been paid to perennial, freshwater, karstic lake systems formed by solution of the sub-surface carbonate or evaporite formations. Although the total area of lakes formed by these processes is less than 1% of total global lake area (Cohen, 2003) and most of them are small, karstic lake basins are numerous in regions such as temperate areas of Southern China, North and Central America (Florida and Yucatán) and the Mediterranean Basin (Spain, Balkans), where carbonate or evaporite lithologies are dominant.

These karstic depressions are generated by dissolution processes, often involving subsidence and/or collapse, thus leading to the generation of funnel-shaped dolines with steep margins, which generally are very deep for their size (Palmquist, 1979; Cvijic, 1981; Gutiérrez-Elorza, 2001; Gutiérrez *et al.*, 2008). This particular morphology, together with the frequent interception of large aquifers, providing considerable groundwater input, leads to the development of relatively deep, perennial and frequently seasonally or annually stratified lake systems, even in semi-arid regions with negative hydrological balances, for example, Lake Zoñar, Southern Spain (Valero-Garcés *et al.*, 2006); Aguelmane Azigza, Atlas Mountains, Morocco (Martin, 1981). The development of these systems on evaporites and carbonate substrates favours sulphate-rich and carbonate-rich water chemical compositions in the case of continental evaporitic bedrocks, e.g. Lac de Besse, France (Nicod, 1999); Lake Demiryurt gölü, Turkey (Alagöz, 1967); Laguna Grande de Archidona, Spain (Pulido-Bosch, 1989); Lago de Banyoles, Spain (Julià, 1980), and generally carbonate-rich and chloride-rich compositions for lakes developed on marine formations, e.g. Lake Vrana, Croatia (Schmidt *et al.*, 2000); Lake Zoñar, Spain (Valero-Garcés *et al.*, 2003).

The relatively small size of these topographically closed basins and the connection to aquifers make these systems very sensitive to regional hydrological balances, experiencing considerable lake level, water chemistry and biological fluctuations in response to changes in effective moisture (Cohen, 2003). In addition, the combination of great depth with multiple episodes of karstification in these endorheic basins can lead to thick deposits with high sedimentation rates providing long, continuous sedimentary sequences with high temporal resolution, suitable for palaeohydrological and palaeoclimate reconstructions [for example, Lago d'Accesa, Italy (Magny *et al.*, 2006, 2007; Millet *et al.*, 2007); Lake Banyoles, Spain (Perez-Obiol & Julià, 1994); Lago di Pergusa, Italy (Sadori & Narcisi, 2001; Zanchetta *et al.*, 2007); Lake Zoñar, Spain (Valero-Garcés *et al.*, 2006; Martín-Puertas *et al.*, 2008)].

The sedimentary sequences from karstic lakes have been used previously for palaeoenvironmental and palaeoclimate analyses. To date, however, no detailed facies models have been defined. Compared with other lacustrine depositional environments (Kelts & Hsü, 1978; Dean, 1981; Dean & Fouch, 1983; Eugster & Kelts, 1983; Wright, 1990; Talbot & Allen, 1996), small karstic lakes show even more abrupt and complex lateral and vertical facies changes. This effect is because internal thresholds of some key factors (e.g. salinity and water chemistry, temperature, light penetration and oxygenation levels) are often modified by extreme events, such as floods (Moreno *et al.*, 2008; Valero Garces *et al.*, 2008) and mass-wasting processes (Bourrouilh-Le Jan *et al.*, 2007). To decipher the high-resolution palaeoenvironmental information archived in these lake sequences, depositional models are required to provide a dynamic framework for integrating all palaeolimnological data (Valero-Garcés & Kelts, 1995).

This paper presents a depositional facies model for small (19 ha) karstic Lake Estanya (North-eastern Spain) that could be applicable to similar modern and ancient sedimentary systems. Previous studies carried out in this lake basin (Wansard *et al.*, 1998; Riera *et al.*, 2004, 2006; Morellón *et al.*, 2008) have shown the potential of this site as a palaeoenvironmental archive but did not resolve the sedimentary evolution of the lake at a basin scale. The use of acoustic, seismic stratigraphy provides a quasi three-dimensional image of the sedimentary basin and direct evidence of major phases of lake-level changes and mass-wasting processes. A facies model has been defined, combining sedimentological features with their mineralogical and organic composition, and blended with the results of an extensive study of present-day depositional environments. Within the framework of this facies model, the relative importance of different factors influencing lake deposition for the last 21 kyr is investigated. Additionally, different proxies for reconstructing past hydrological changes in karstic systems are evaluated.

REGIONAL SETTING

Geological and geomorphological setting

'Balsas de Estanya' (42°02′ N, 0°32′ E; 670 m above sea-level) is a karstic lake complex located at the foothills of the Sierras Exteriores, the External Pyrenean Ranges in Northern Spain (Martínez-Peña & Pocoví, 1984). The External Pyrenean Ranges are composed of Mesozoic formations with east–west trending folds and thrusts. Outcrops of Upper Triassic carbonate and evaporite formations along these structures have favoured karstification processes and the development of large poljes and dolines (IGME, 1982). The Balsas de Estanya lake complex is located in a relatively small endorheic basin of 2·45 km^2 (López-Vicente, 2007) (Fig. 1A and B) that belongs to a larger Miocene polje structure (Sancho-Marcén, 1988). An Upper Triassic low-permeability marl and claystone formation (Keuper facies) constitutes the lake basin substrate whereas Mid Triassic limestones and dolostone Muschelkalk facies outcrops make up the higher reliefs of the catchment (Sancho-Marcén, 1988). The karstic system consists of three dolines with water depths of 7 m, 20 m and one that is only seasonally flooded. Furthermore, a number of karstic depressions filled with Quaternary sediments also occur (IGME, 1982; Sancho-Marcén, 1988; López-Vicente, 2007).

Climate and hydrogeology

The region has a Mediterranean continental climate characterized by a long summer drought (León-Llamazares, 1991). The mean annual temperature is 14 °C with monthly means ranging from 4 °C (January) to 24 °C (July). Mean annual rainfall is 470 mm whereas the mean annual evapotranspiration rate has been estimated as 774 mm (Meteorological Station at Santa Ana Reservoir, 17 km south-east of the lake). July is the driest month with an average rainfall of 18 mm and October is the most humid month (50 mm).

The main lake basin, 'Estanque Grande de Abajo' (42°02′ N, 0°32′ E, 670 m a.s.l.), is an uvala formed by the coalescence of two sub-basins with maximum water depths of 12 and 20 m and steep margins (Ávila *et al.*, 1984). These two sub-basins are separated by a sill, 2 to 3 m below the present-day lake level, which only emerges during prolonged dry periods, for example, during the 1994 to 1996 drought (Morellón *et al.*, 2008). The total lake surface is 188 306 m^2, with a maximum length of 850 m and a maximum width of 340 m. Total volume has been estimated as 983 728 m^3 (Ávila *et al.*, 1984).

The 'Estanque Grande de Abajo' has a relatively small watershed [106·50 ha surface (López-Vicente, 2007)]. Although there is no permanent

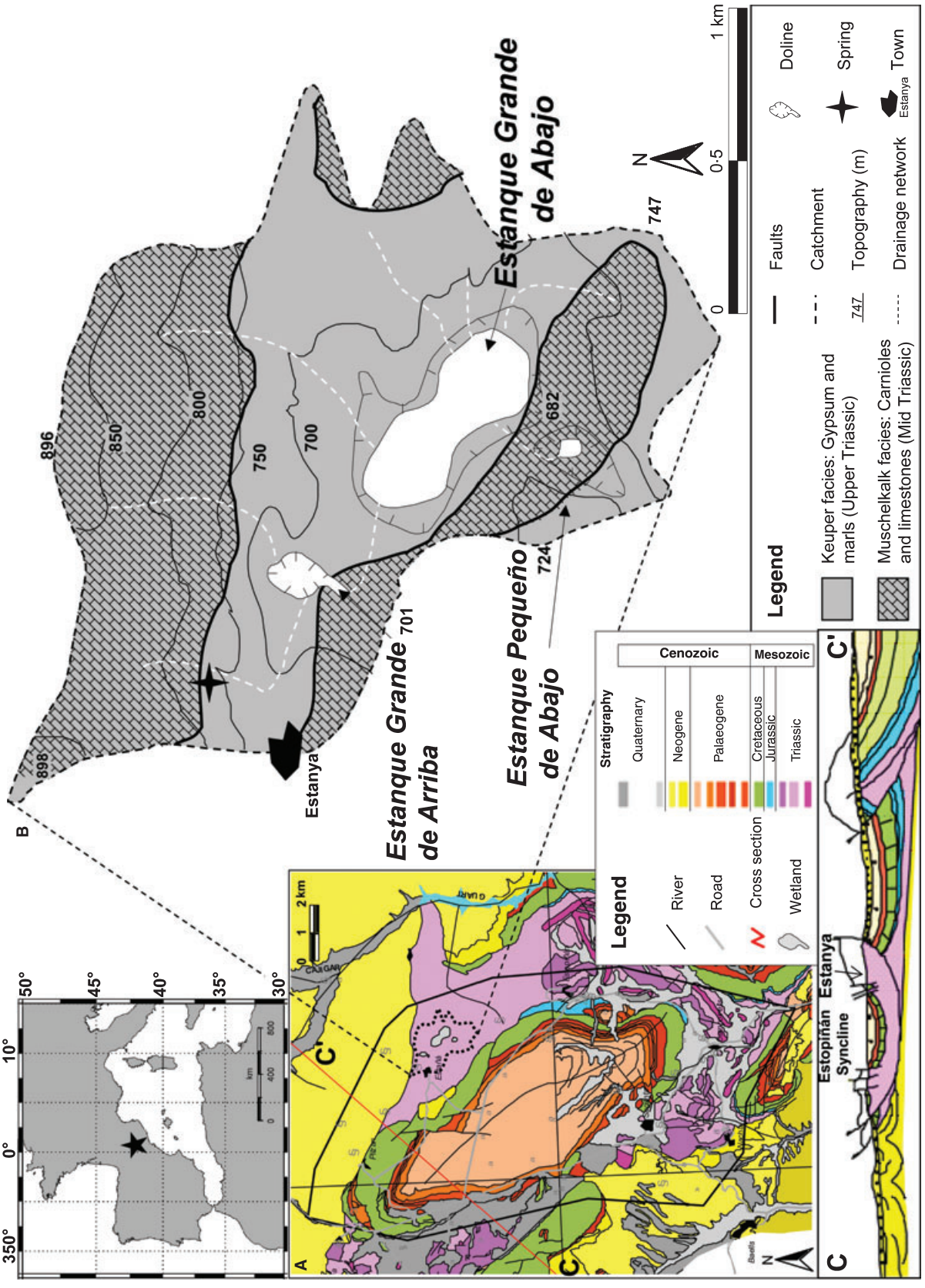

Fig. 1. Location map of *Balsas de Estanya* karstic lake system: (A) geological map and cross-section (C–C') of the Estopiñán Syncline (main hydrogeological system in the area) and surroundings (modified from Villa & Gracia, 2004); (B) topographic and geological map of Balsas de Estanya catchment (see legend below).

inlet, several ephemeral creeks drain the catchment providing clastic material to the lake during extreme precipitation events; alluvial and colluvial deposits occur in the northern and eastern littoral areas (López-Vicente, 2007). Archaeological evidence indicates that there has been water management in the area since the 12th Century (Riera *et al.*, 2004, 2006). An artificial canal feeds the main lake when the water capacity of the small lake is exceeded. However, given the low water volume provided by this canal, it is discarded as a significant input to the lake.

There is no surface outlet and the nature of the substrate, composed of low permeability Upper Triassic Keuper facies, limits groundwater losses. Consequently, modern hydrology of Lake Estanya is controlled mostly by groundwater inputs and evaporation output. Calculated evapotranspiration exceeds rainfall by about 300 mm year^{-1}. The lake is fed mainly by groundwaters from the surrounding local dolostone aquifer (Muschelkalk), probably related to the hydrogeological system of the Estopiñán Syncline (Villa & Gracia, 2004). A permanent spring (0·3 l sec^{-1}) (Villa & Gracia, 2004) is located at the north end of the polje feeding the small Estanque Grande de Arriba (Fig. 1B). There are no available groundwater and lake level data to calculate the hydrological balance in the lake. However, the response of the system to precipitation is relatively rapid, as indicated by the observed *ca* 1 m lake-level drop during the relatively dry year 2005, and by the 2 to 3 m lake-level drop during the previous long dry period 1994 to 1996 when the central sill separating the two sub-basins emerged (Morellón *et al.*, 2008).

Limnology

Lake water is brackish (electrical conductivity, 3200 μS cm^{-1} and total dissolved solids (TDS), 3400 mg l^{-1}), and sulphate and calcium-rich: [SO_4^{2-}] > [Ca^{2+}] > [Mg^{2+}]> [Na^{+}]. The lake is monomictic, with thermal stratification and anoxic hypolimnetic conditions during spring and summer, extending from March to September, and oligotrophic (Ávila *et al.*, 1984) (Table 1). Vertical profiling in September 2007 revealed thermal stratification with a thermocline located at 6 to 9 m water depth (Fig. 2, Table 1). The higher electrical conductivity in the epilimnion indicates the relative importance of evaporation loss. Differences in water chemistry with the nearby Estanya Spring (Table 1) also suggest a long residence time and a major influence of

Table 1. Physical and chemical properties of the Estanya Spring and Lake Estanya (south-east sub-basin) at the lake surface and 16 m water depth for 24 June 2005 (summer stratification season).

Sample	Water depth (m)	Temperature (°C)	Conductivity (μS cm^{-1})	pH	Oxygen saturation (%)	Mg (mg l^{-1})	K (mg l^{-1})	Na (mg l^{-1})	Sr (mg l^{-1})	Li (mg l^{-1})	Ca (mg l^{-1})	HCO_3 (mg l^{-1})	Cl (mg l^{-1})	SO_4 (mg l^{-1})
Estanya Spring	–	14·0	627	7·64	100·0	12·7	1·7	20·5	0·23	0·11	55·3	0·3	1·2	48·5
Lake Estanya	0	24·3	3 440	7·63	65·8	132	14·2	133	7·8	0·16	440	1·37	6·6	1813·1
Lake Estanya	16	5·1	3 330	7·39	0·0	127	14	124	7·1	0·15	402	1·49	6·3	–

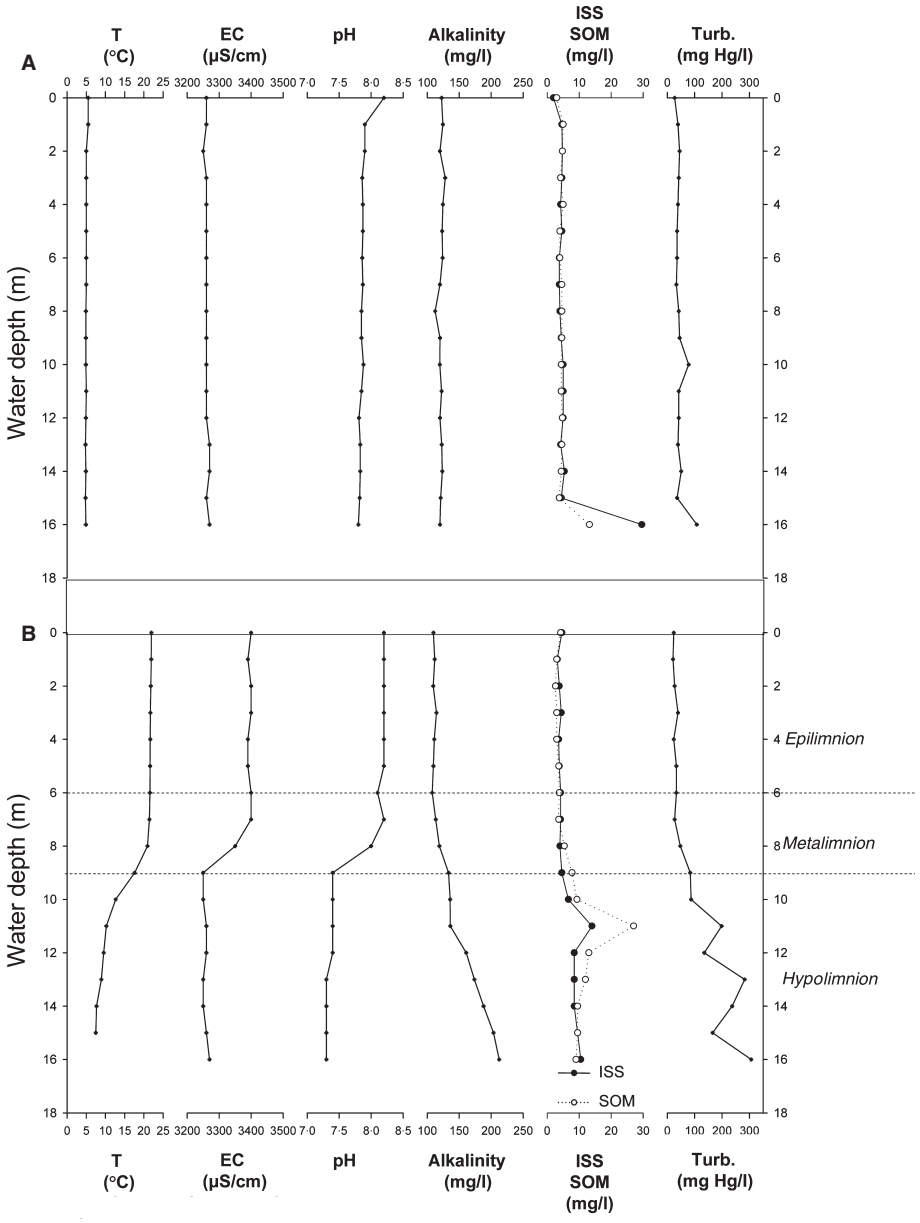

Fig. 2. Physical–chemical vertical profiles of the water column at the deepest area of *Estanque Grande de Abajo*. (A) Vertical profile measured in January 2008 (winter mixing period); (B) vertical profile measured in September 2007 (summer stratification period). From left to right: *T* (°C), temperature; EC (µS cm^{-1}), electrical conductivity; pH; alkalinity (mg l^{-1}); ISS (mg l^{-1}), inorganic suspended solids; SOM (mg l^{-1}), suspended organic matter; Turb. (mgHg l^{-1}), turbidity.

evaporation on the system, as pointed out by previous studies (Villa & Gracia, 2004). An additional vertical profile measured in February 2008 revealed a well-mixed water column with homogeneous thermal and oxic conditions throughout (Fig. 2A). Suspended solids are higher during the summer season (Fig. 2B) revealing an important contribution of clastic material derived from the erosion of soils after the harvest (López-Vicente *et al.*, 2008). Anoxic hypolimnetic conditions during the summer stratification period favour organic matter (OM) preservation, as indicated by the increase in the relative amount of suspended OM with respect to the inorganic suspended sediments below 9 m water depth (Fig. 2B). Sulphide precipitation is favoured by the activity of sulphate-reducing bacteria (SRB) in the hypolimnion (Esteve *et al.*, 1983; Guerrero *et al.*, 1987; Mir-Puyuelo, 1997; Ramírez-Moreno, 2003). Maximum alkalinity values in the epilimnion are reached in the summer season, coinciding with the maximum algal productivity (Fig. 2B). During

this season, alkalinity increases with increasing water depth, as a result of dissolution of carbonates at the hypolimnion, where pH is lowered by SRB-derived sulphide input (Ávila *et al.*, 1984).

MATERIALS AND METHODS

The Lake Estanya watershed was identified and mapped using topographic and geological maps and aerial photographs. Both lake sub-basins were geophysically surveyed in June 2002 using a high-resolution, single-channel seismic system with a centre frequency of 3·5 kHz (GeoAcoustic pinger source) of the ETH-Zürich (Zürich, Switzerland). The source/receiver was mounted on a catamaran raft that was pushed by a boat. The studied basins were covered with a dense grid of *ca* 6 km of seismic lines providing a mean spatial resolution of *ca* 50 m between each line. Seismic-processing workshop software was used for processing of the data (bandpass filter, water bottom mute) and the resulting seismic data set was interpreted using the KINGDOM SUITE software (Seismic Micro Technology-Europe Ltd, Croyden, UK).

Surface sediments were sampled with a Uwitec© short-corer (Uwitec, Mondsee, Austria) at 34 selected points distributed in a grid covering all present-day depositional environments. The uppermost 1 cm of each short core was sampled and sediment aliquots were sub-sampled for different analyses. Grain-size was determined using a Coulter particle-size analyser (Beckman Coulter Inc, Fullerton, CA, USA) (Buurman *et al.*, 1997). Samples were treated with 10% hydrogen peroxide in a water bath at 80 °C to eliminate the OM; a dispersant agent and ultrasound treatment were used prior to measurement. Total organic carbon (TOC) and total inorganic carbon (TIC) were measured with a LECO SC 144 DR elemental analyser (LECO Corporation, St Joseph, MI, USA) and total nitrogen (TN) with a VARIOMAX CN (Elementar Analysensysteme GMBH, Hanau, Germany). Whole sediment mineralogy was characterized by X-ray diffraction with a Philips PW1820 diffractometer (Philips Analytical, PANalytical B.V., Almelo, the Netherlands) and relative mineral abundance was determined using peak intensity following the procedures described in Chung (1974a,b). Mapping of different sediment properties through the lake floor was carried out with ARCMAP 9.0® (ESRI Corporate Headquarters, Redlands, CA, USA), using the inverse distance weighted (IDW) interpolation tool.

Coring operations were conducted in two phases: four cores were retrieved in 2004 using modified Kullenberg piston coring equipment and platform from the Limnological Research Center (LRC) (University of Minnesota, Minneapolis, MN, USA) and an additional Uwitec© piston core (Uwitec) was recovered in 2006. The longest cores (1A-1K and 5A-1U) reached 4·5 and 11 m below the lake floor, respectively.

Physical properties (magnetic susceptibility and density) were measured in all cores with a Geotek Multi-Sensor Core Logger (MSCL; Geotek Limited, Daventry, UK) every 1 cm. The cores were subsequently split into two halves and imaged with a DMT Core Scanner (DMT GmbH & Co KG, Essen, Germany) and a GEOSCAN II digital camera (Geotek Limited). Sedimentary facies were defined after visual, microscopic observation of smear slides in both superficial sediment and in the core samples, following the methodology described in Schnurrenberger *et al.*, 2003.

Cores were sub-sampled every 2 cm for TOC and TIC and every 5 cm for mineralogical analyses following the methodology described above. Scanning electron microscope images were taken under low-vacuum conditions in an environmental scanning electron microscope on uncoated fragment samples. Backscattered electron images were obtained in order to see compositional differences of the components as grey-level contrast. Images reflect the average chemical composition of grains with the darker grains being made-up of lighter elements than the brighter grains. In addition, energy dispersive X-ray spectrometric analysis (Phoenix system; EDAX, Mahwah, NJ, USA) was performed when necessary.

The chronology for the lake sequence is constrained by 17 accelerator mass spectrometry (AMS) ^{14}C dates analysed at the Poznan Radiocarbon Laboratory (Poznan, Poland) (Tables 2 and 3). Although most of the dated samples correspond to terrestrial macro-remains, in eight samples bulk OM was analysed because of the absence of organic rests. The reservoir effect was calculated after dating pairs of bulk OM samples and terrestrial organic macrorests at three depth intervals representative of different sediment compositions and time-periods (Table 2). The correction was applied to dates not derived from macrorests. Corrected radiocarbon dates were calibrated using CALPAL_A software and the INTCAL04 curve (Reimer *et al.*, 2004), selecting the median of the 95·4% distribution (2σ probability interval). The age–depth relationship was

estimated by means of a generalized mixed-effect regression (Heegaard *et al.*, 2005).

RESULTS

Seismic stratigraphy

Seismic penetration into the sub-surface down to the acoustic basement allowed tracking of the bedrock morphology in most parts of the lake. Sediment thickness reaches up to *ca* 15 m in both sub-basins with two depocentres occurring at the deepest areas. Seismic stratigraphic analysis allowed the identification of three major seismic units ('A' to 'C'; Fig. 3A) and several seismic horizons, which have been tracked through the basins. These horizons and units were correlated with the core lithostratigraphy. A constant acoustic velocity of 1500 m sec^{-1} based on the MSCL measurements has been used for the seismic-to-core correlation (Fig. 3A).

The bedrock surface is locally irregular and marked by discrete steps and sharp edges, prob-

Table 2. Comparison between pairs of radiocarbon dates obtained after analyzing bulk organic sediment and plant macro-remains at the same core depth intervals.

Core	Comp. depth (cm)	Laboratory code	Type of material	^{14}C AMS age (yr BP)	Calculated reservoir effect (^{14}C years)
1A	35·5	Poz-24749	*Phragmites* stem	155 ± 30	
		Poz-24760	Bulk organic matter	740 ± 30	585 ± 60
	439·5	Poz-9891	Wood fragment	8510 ± 50	
		Poz-23670	Bulk organic matter	9330 ± 50	820 ± 100
5A	890·6	Poz-17194	Wood fragment	16100 ± 80	Reworked
		Poz-23671	Bulk organic matter	15160 ± 90	(*)

The calculated reservoir effect is indicated for each of the bulk organic matter samples.
*The negative reservoir effect obtained in this sample (−940 ± 170) is because of the reworked nature of the terrestrial organic macrorest. [Comp. = composite]

Table 3. Radiocarbon dates used for the construction of the age model for the Lake Estanya sequence. A correction of −820 ± 100 ^{14}C years was applied to bulk sediment samples from Units II to VI. Corrected dates were calibrated using CALPAL_A software and the INTCAL04 curve (Riera *et al.*, 2004); and the mid-point of 95·4% (2σ probability interval) was selected.

Comp. depth (cm)	Laboratory code	Type of material	AMS ^{14}C age (yr BP)	Corrected AMS ^{14}C age (yr BP)	Calibrated age (cal yr BP) (range 2σ)
Core 1A					
35·5	Poz-24749	*Phragmites* stem fragment	155 ± 30	155 ± 30	160 ± 100
61·5	Poz-12245	Plant remains and charcoal	405 ± 30	405 ± 30	460 ± 60
177	Poz-12246	Plant remains	895 ± 35	895 ± 35	840 ± 60
196·5	Poz-15972	Bulk organic matter	2120 ± 30	1300 ± 130	1210 ± 130
240	Poz-12247	*Salix* leave	3315 ± 35	3315 ± 35	3550 ± 50
337·5	Poz-12248	*Graminea* seed	5310 ± 60	5310 ± 60	6100 ± 90
350	Poz-15973	Bulk organic matter	6230 ± 40	5410 ± 140	6180 ± 150
390	Poz-15974	Bulk organic matter	8550 ± 50	7730 ± 150	8600 ± 180
439·5	Poz-9891	Wood fragment	8510 ± 50	8510 ± 50	9510 ± 30
Core 5A					
478·6	Poz-17190	Plant macroremain	8830 ± 50	8830 ± 50	9940 ± 150
549·6	Poz-17191	Bulk organic matter	10 680 ± 60	9860 ± 160	11 380 ± 270
614·6	Poz-20138	Bulk organic matter	11 820 ± 60	11 000 ± 160	12 980 ± 120
659·6	Poz-17192	Macroremain	11 710 ± 60	11 710 ± 60	13 570 ± 90
680·1	Poz-20139	Bulk organic matter	12 700 ± 70	11 880 ± 170	13 730 ± 190
704·1	Poz-20067	Bulk organic matter	13 280 ± 60	12 460 ± 160	14 550 ± 300
767·6	Poz-17283	Bulk organic matter	14 830 ± 90	14 010 ± 190	16 730 ± 270
957·5	Poz-20140	Plant remains	15 130 ± 100	15 130 ± 100	18 420 ± 220

ably reflecting the karstic origin of the two depressions. Overlying the acoustic basement, Seismic unit 'C' is characterized by low-amplitude reflections that are mostly continuous and intercalated with seismically transparent units. Based on this pattern, a rather homogeneous sediment composition is assumed lacking major impedance contrasts (Fig. 3A). Only few medium-amplitude reflections occur towards the top of the unit, coinciding with the density contrasts caused by alternating gypsum-rich and clastic lithologies. The thickness of seismic unit 'C' is highly variable reaching up to 10 m towards the depocentres of both sub-basins, whereas it is nearly absent in proximal areas of the basin and on the sill.

Seismic unit 'B' is characterized by closely spaced high-amplitude reflections, increasing upwards as a result of more frequent lithological changes towards the top of the unit. Correlation with core lithostratigraphy shows that the high number of reflections corresponds to the physical contrast between alternating gypsum beds (high density) with organic-rich lithologies (low density) containing massive silts. Well-defined parallel reflections are more common in distal areas probably representing more clastic and finer facies, whereas alternating parallel-to-chaotic seismic facies are found in proximal areas, probably reflecting a more dynamic sedimentation affected by truncation surfaces as a result of alternating deposition and erosion cycles. The general sediment geometry, characterized in underlying unit 'C' by a ponding style, changes in unit 'B' to a draping pattern, so that unit 'B' covers most of the lake with a maximum thickness of *ca* 4 m.

Seismic unit 'A' is characterized by varying seismic facies ranging between low-amplitude to high-amplitude reflections that are all laterally continuous. The corresponding lithologies observed in the core comprise rather homogenous clastic and fine-grained sediments with a few thin intervals rich in plant debris and coarser-grained centimetre-thick intercalations. The latter are more frequent in the south-eastern sub-basin which explains the higher amplitudes of seismic reflections when compared with the north-western sub-basin. Unit 'A' is also of a draping geometry with a thickness of up to *ca* 3 m, reaching far into the littoral areas of the lake.

The seismic survey identified several small mass-wasting deposits, particularly in the south-eastern sub-basin. The largest mass-wasting deposit is restricted to the north-eastern margin of the south-eastern sub-basin, and has a characteristic mound-shaped morphology, with an irregular lower surface, a slightly hummocky upper surface and a lobe-shaped distal termination (Fig. 3A). The internal structure is characterized by chaotic to transparent seismic facies, typical of mass flows (Mitchum *et al.*, 1977; Coleman & Prior, 1988; Schnellmann *et al.*, 2005). The maximum lateral extent of this deposit is *ca* 150 m and its maximum thickness reaches *ca* 5 m. Seismic-to-core correlation of the horizon picked on the top of the mass-flow deposit shows that it occurred around the transition between seismic units 'A' and 'B' (*ca* 800 cal yr BP, according to the age model in this study). Similar mass flow deposits also occur within seismic unit 'C', mostly in the north-western sub-basin (Fig. 3A).

The change in sedimentation style through time reflects large changes in the lake system. The thinning and onlapping of unit 'C' towards the slopes and sill areas suggest that the two sub-basins were not permanently connected during the early stages of basin evolution. Although sediment-focusing processes due to lateral sediment transport may have contributed to this sediment geometry, this pattern is more probably a reflection of predominating isolation of both sub-basins during this initial lake stage. In contrast, the rather constant thickness of units 'A' and 'B' throughout the basin result in draping geometries and wider lateral extent, as well as the good lateral correlation of reflections between the two sub-basins, indicating that they have been predominantly connected during deposition of those units. The deposition of unit 'A' is not only laterally continuous throughout the lake basin but shows a similar thickness in the littoral areas, pointing to a regular and stable sedimentation over the entire lake area in recent times. The limited lateral changes in seismic facies of unit 'A', however, can be related to the present-day distribution of depositional sub-environments in the lake basin (Fig. 3A).

Sedimentary facies and depositional environments

Present-day sedimentary facies and depositional sub-environments

Sedimentary facies in modern Lake Estanya were described and interpreted based on 34 sampling points (Fig. 4). The relatively small size of the lake, its topographically closed watershed and its double funnel-shaped morphology (López-Vicente, 2007) determine the present low-energy

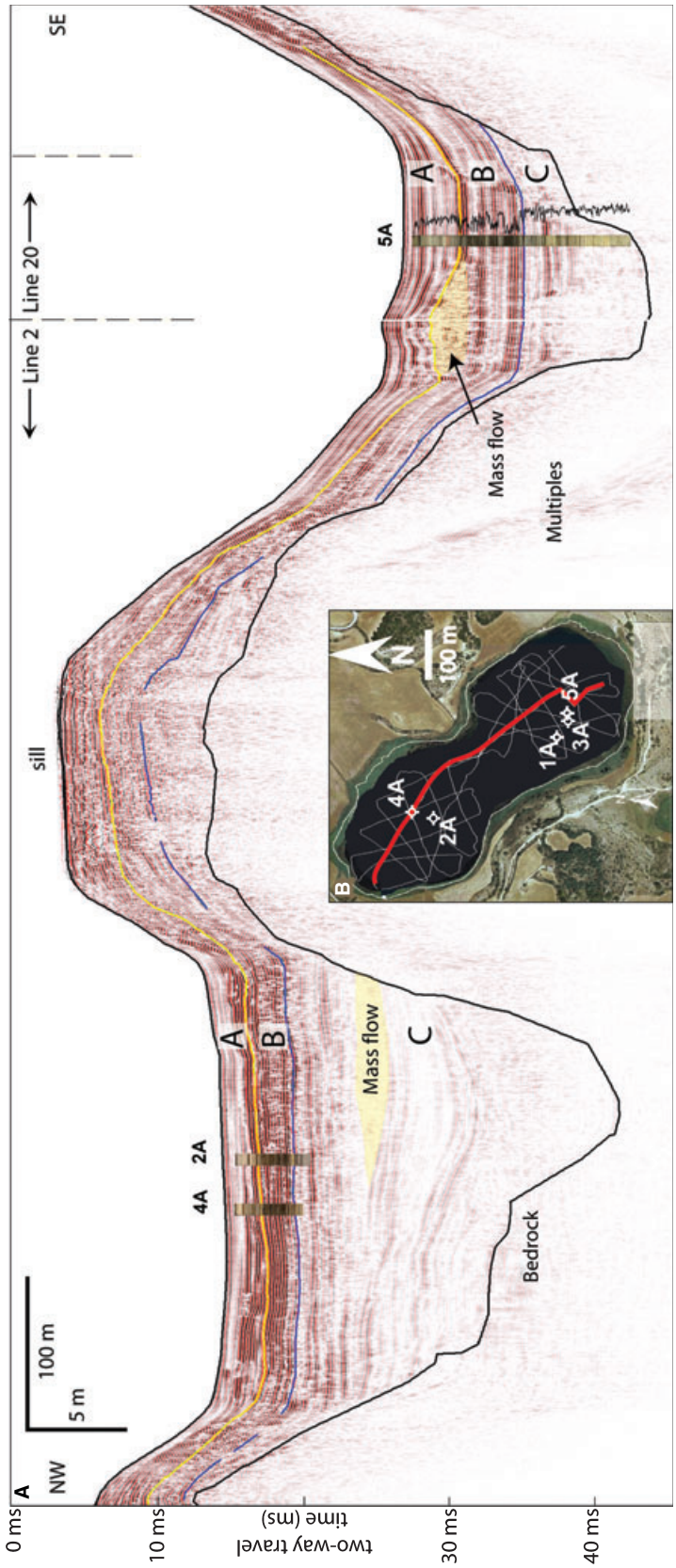

Fig. 3. (A) NW–SE seismic section (connecting Line 2 and Line 20) crossing both sub-basins and the sill. Note the two kinks in the track marked by dashed lines on top. Three seismic units ('A' to 'C') can be identified in the sedimentary succession overlying the basement. Correlation with cores 2A, 4A and 5A is also indicated by superposition of core images and additionally a density (g cm^{-3}) profile for core 5A. (B) The inset map shows the seismic grid overlain on an aerial photograph with an indication of the long-core locations.

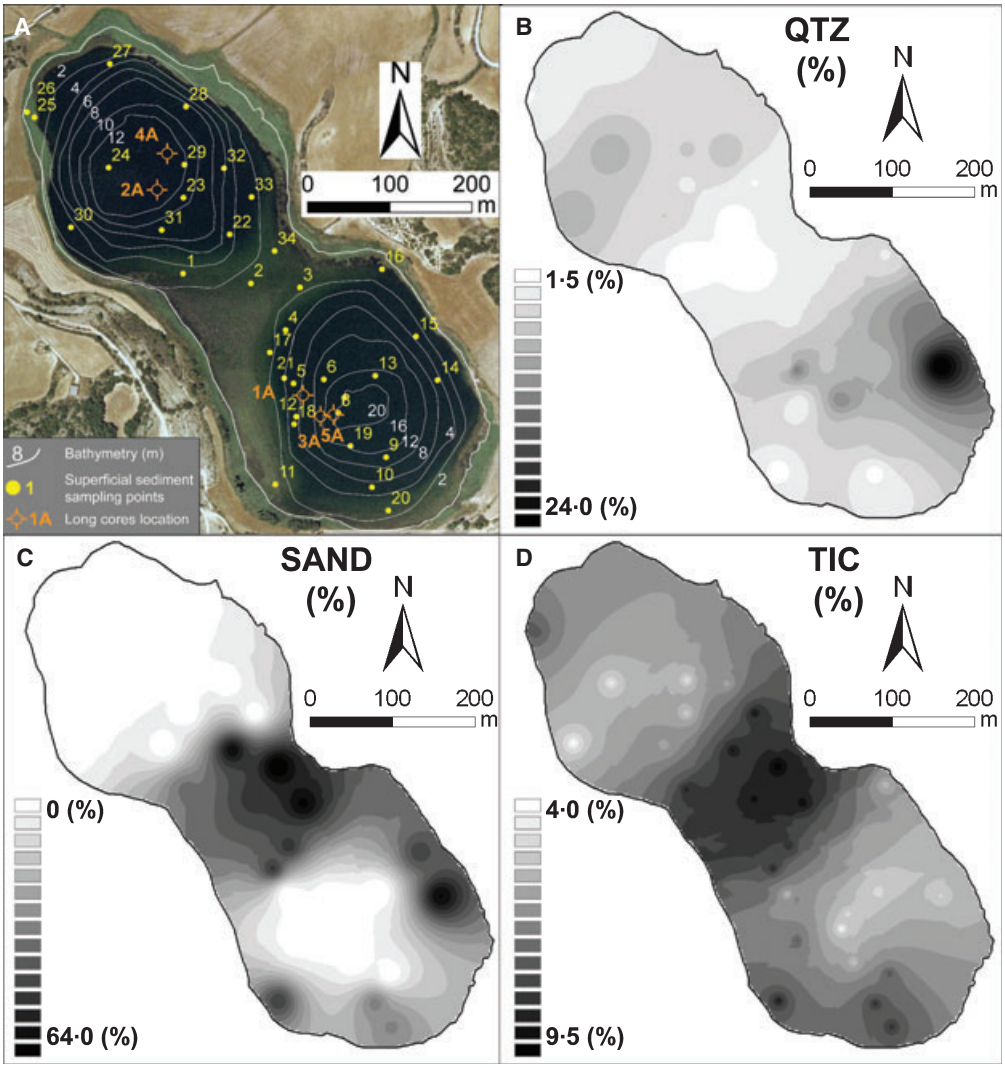

Fig. 4. (A) Aerial photograph, bathymetry (modified from Ávila *et al.*, 1984) and distribution of superficial sediment sampling points and long cores recovered in Lake Estanya, accompanied by density maps of: (B) quartz (Qtz) content (%), (C) sand content (%) and (D) total inorganic carbon (TIC) content (%). Interpolation method used for mapping was inverse distance to weight (IDW) (ARCMAP 9.0®) and 15 different classes defined at equal intervals from minimum to maximum values for each case, were considered (see greyscale legends).

depositional environments, relatively small lake-level fluctuations (2 to 3 m) and the development of seasonal anoxia in the deepest areas. The modern lake could be described as a freshwater to brackish, relatively deep, carbonate-producing, monomictic lake, with some similarities to the carbonate lake models described by Murphy & Wilkinson (1980) and Platt & Wright (1991). According to sedimentological features, grain-size distribution, mineralogical content and OM composition, three main depositional sub-environments can be identified in the modern lake basin (Fig. 5A): (i) the littoral platform; (ii) the transitional area; and (iii) the offshore, distal area.

(i) The 'littoral platform' constitutes a flat area, partially colonized by vegetation that protects the littoral zones from waves, stabilizes the substrate, provides support for epiphytic fauna and largely contributes to the production of carbonate particles. This sub-environment is better developed along the southern shores and in the sill, which are both characterized by gentle slopes, and it is spatially restricted to a narrow strip on the steep northern shore (Fig. 5A).

The 'internal littoral platform' is a 5 to 10 m wide area extending from the inner limit of the littoral vegetation belt (*Juncus* sp., *Tamarix* and *Phragmites australis*) to the modern lake shoreline. This area is only occasionally submerged

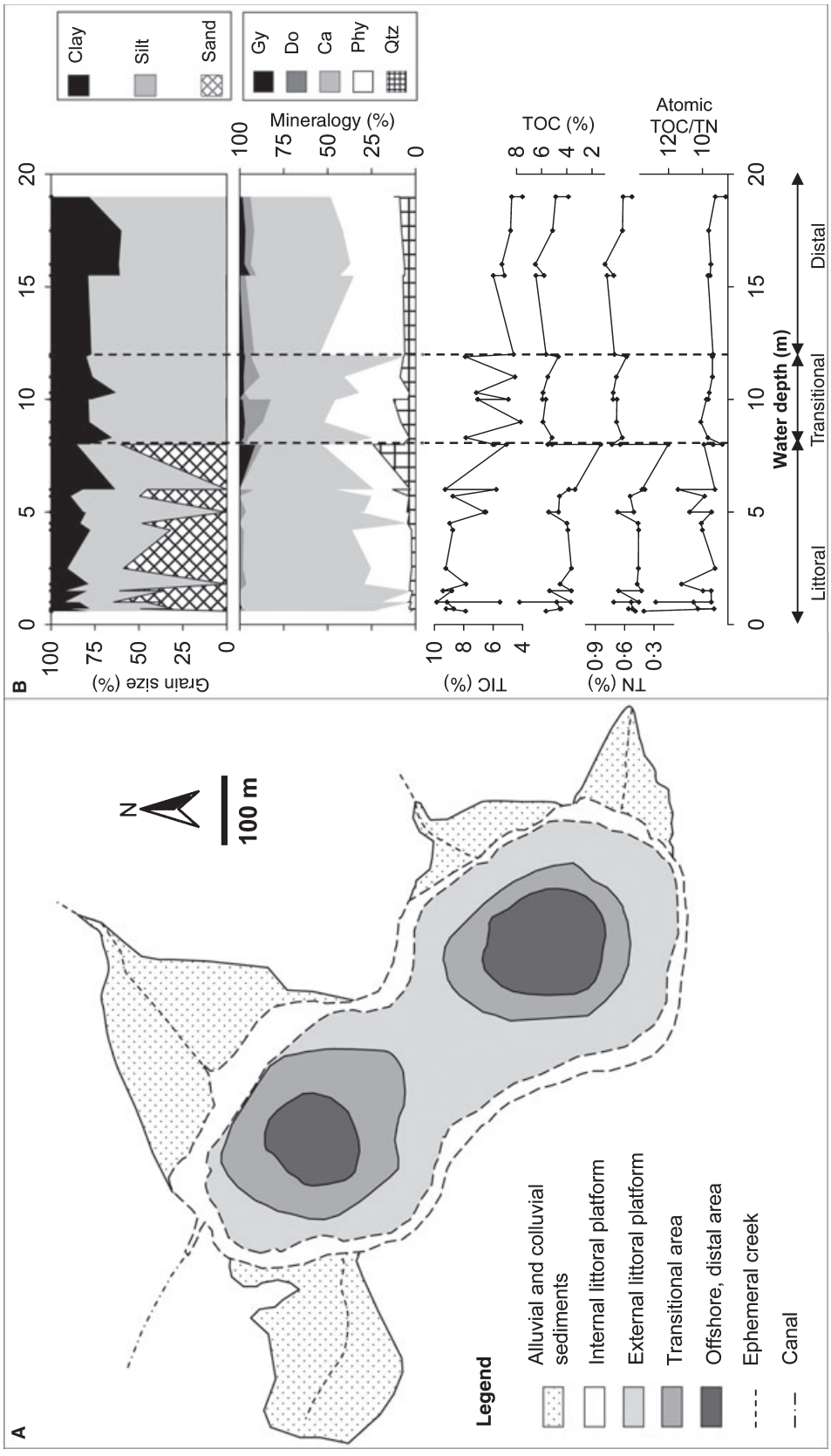

Fig. 5. (A) Depositional sub-environments identified in Lake Estanya. (B) Changes in sediment properties (*Y*-axis) in respect of water depth (m) (*X*-axis). From top to bottom: grain-size (expressed as percentages of sand, silt and clay fractions), bulk mineralogy [expressed as percentages of quartz (Qtz), phyllosilicates (Phy), calcite (Ca), dolomite (Do) and gypsum (Gy) (see legend); TIC (%)-total inorganic carbon, TOC (%)-total organic carbon, TN (%)-total nitrogen; atomic TOC/TN-total organic carbon/total nitrogen ratio. Depositional sub-environments corresponding to each water-depth interval have also been indicated at the bottom of the panel.

during periods of high lake level. Sediment is composed mainly of light grey, massive, bioturbated (root casts, worm tracks and mixed sediment textures) coarse silts with abundant plant remains.

The 'external littoral platform' (0 to 4·5 m water depth) corresponds to the permanently submerged, shallow area located between the shoreline and the slope. This area has a mean width of 50 m around the two sub-basins but reaches a width of 200 m on the sill. The proximal areas of this sub-environment are colonized by submerged macrophytes and charophyte meadows which extend offshore. This environment is the main carbonate factory in the lake, comprising biogenic carbonates (ostracods, gastropods and *Chara* sp. particles) and non-biogenic carbonates (coatings around submerged macrophytes and the lake substrate). Precipitation of small calcite crystals in the epilimnion associated with algal blooms seems to be a smaller contributor to the total carbonate production in the lake. Storms and wave activity lead to the reworking of these particles, as indicated by the occasional presence of ripples in some areas. Sediment is composed mainly of banded to massive yellowish/light grey, bioturbated carbonate-rich (6 to 10% TIC) silts to fine-grained sands (averaging 100 μm) with plant remains (< 4% TOC).

(ii) The 'transitional talus' (from 4·5 to 8 m water depth) is a narrow area (< 25 m wide) characterized by steep morphology, limited presence of vegetation as a result of the lack of light (Ávila *et al.*, 1984) and the occurrence of small mass movements as a result of talus destabilization. Carbonates originating in the littoral platform are transported to the talus. Sediments are dark grey massive silts (averaging 10·5 μm) with carbonates. Mass-wasting processes remobilize talus sediments and transport fine detrital material downslope to distal areas.

(iii) The 'offshore, distal area' (from 8 to 19 m water depth) comprises the central, deepest and relatively flat areas characterized by black, massive to laminated fine-grained silts (averaging 10·1 μm). Sediments are transported as suspended load to distal areas and by occasional mass-wasting processes. The presence of carbonates is limited (< 5% TIC) because of the large distance to the producing littoral areas and to the dissolution processes that remove small carbonate particles. This sub-environment is affected by seasonal anoxic hypolimnetic conditions (Ávila *et al.*, 1984) and, thus, bioturbation processes are greatly reduced or absent. The presence of SRB previously reported by numerous studies at this site (Esteve *et al.*, 1983; Guerrero *et al.*, 1987; Mir-Puyuelo, 1997; Ramírez-Moreno, 2003) favours sulphide formation in the summer season and is responsible for the characteristic dark colour of the sediments and relatively high OM preservation (4 to 6% TOC). Although the mixing period of the water column may last from September to March (Ávila *et al.*, 1984), the footprint of summer anoxic conditions with prevailing oxygen and light-depleted conditions, characterizes the deeper sediments. Oxic/anoxic cycles are only locally recognized at some sampling points where alternating black and dark grey laminations are observed.

Lake basin topography, water depth and distance to shore appear to be the main factors controlling the distribution of present-day surface sediments in the lake. Grain-size obviously is controlled by the distance to shore, showing a decreasing trend towards the distal areas (Figs 4 and 5B). Carbonates are more abundant in the littoral and transitional areas and less abundant in the deepest areas, in part due to dissolution processes and distance to shore. Organic matter content in the littoral platform decreases towards the transitional area and it is a mixture of terrestrial, submerged macrophytes and algal material. The organic content increases again in distal areas as a result of the higher preservation potential provided by seasonally anoxic conditions. Distal OM is characterized by comparatively low atomic TOC/TN ratios (9·3 versus 10·4) indicating a higher contribution of algal sources (Meyers, 1997; Meyers & Lallier-Vergès, 1999).

Core sedimentary facies

Ten facies have been defined and correlated within the five long sediment cores recovered at the offshore, distal areas of the two Lake Estanya sub-basins, based on detailed sedimentological descriptions, smear-slide microscopic observations and compositional analyses. According to compositional criteria, these facies have been grouped into four main categories as: (i) clastic; (ii) organic-rich; (iii) carbonate-rich; and (iv) gypsum-rich facies (Table 4A, Fig. 6A).

The clastic facies includes banded to laminated, silty and clayey sediments composed of clay minerals, calcite and quartz, with minor amounts of dolomite, feldspars, high magnesium calcite (HMC), pyrite and occasionally gypsum and aragonite. Organic content is relatively low, although with a large range (1 to 7% TOC) and comprises amorphous lacustrine OM, diatoms

Table 4. Main sedimentological and mineralogical features, compositional parameters (TIC, TOC, TN and TOC/TN ratio, expressed as minimum to maximum intervals) and inferred depositional environments and sub-environments for the different facies and sub-facies defined for: (A) Lake Estanya sedimentary sequence (modified from Morellón *et al.*, 2008); (B) present-day depositional sub-environments and equivalent facies in the core sequence.

(A)

Facies		Sedimentological features		Compositional parameters	Depositional subenvironment
Clastic facies	1	**Blackish, banded carbonate clayey silts** Clay-rich matrix mainly composed of phyllosilicates and silty fraction composed of calcite, quartz and dolomite. Minor amounts of feldspars, high-magnesium calcite (HMC) and gypsum. Frequent biogenic components as aggregates of amorphous lacustrine organic matter, macrophyte remains and diatoms.		**TIC** = 1·95 to 3·60% **TOC** = 2·25 to 7·40% **TN** = 0·25 to 0·70% **TOC/TN** = 6·90 to 11·2	Deep, monomictic, seasonally stratified freshwater to brackish lake
	2	**Grey, banded to laminated calcareous silts** Calcite, quartz and dolomite silt-sized particles embedded in a clay-rich matrix. Minor amounts of feldspars, HMC, pyrite and gypsum. Presence of biogenic components: diatoms, amorphous lacustrine organic matter and land-derived plant remains (frequent).	**Subfacies 2.1:** decimetre-thick, laminated to banded intervals with regular, sharp contacts	**TIC** = 1·50 to 4·25% **TOC** = 0·85 to 4·20% **TN** = 0·10 to 0·45% **TOC/TN** = 6·15 to 15·5	Deep, monomictic, seasonally stratified, freshwater to brackish lake
			Subfacies 2.2: centimetre-thick to millimetre-thick laminae with diffuse and irregular contacts, constituted by massive, graded sediments.		Flood and/or turbiditic events
	3	**Black, massive to faintly laminated silty clay** Clay-rich matrix dominant, with silt-sized calcite and quartz particles and frequent amorphous lacustrine organic matter aggregates. Minor amounts of dolomite, feldspars, HMC and gypsum.		**TIC** = 2·15 to 3·10% **TOC** = 0·95 to 2·10% **TN** = 0·10 to 0·2% **TOC/TN** = 7·40 to 10·5	Deep, dimictic, freshwater lake

Table 4. (*Continued*)

Facies	Sedimentological features	Compositional parameters	Depositional subenvironment
Organic-rich facies	4 **Brown, massive to faintly laminated sapropel with gypsum** Organic sediments are composed of amorphous lacustrine organic matter, diatoms and some macrophyte remains, with minor amounts of clay minerals, calcite, dolomite and quartz. Gypsum laminae are composed of idiomorph, well-developed crystals ranging from 25 to 50 μm; millimetre to 1 cm-sized nodules also occur within the sediment	**TIC** = 0 to 11·55% **TOC** = 0·90 to 24·3% **TN** = 0·05 to 1·95% **TOC/TN** = 5·35 to 25·45	Shallow saline lake
	5 **Variegated finely laminated microbial mats with aragonite and gypsum** Sets of dark-brown laminae (lacustrine organic matter, diatoms), yellowish millimetre-thick laminae (authigenic carbonates (calcite, aragonite, dolomite), and occasional grey carbonate silt laminae.	**TIC** = 0 to 8·30% **TOC** = 5·35 to 21·5% **TN** = 0·50 to 1·75% **TOC/TN** = 9·05 to 21·5	Moderately deep saline lake with light penetration
Carbonate-rich facies	6 **Grey and mottled, massive carbonate silt with plant remains and gypsum** Calcite is dominant, followed by clay minerals, dolomite and quartz and minor amounts of HMC and gypsum. Gypsum nodules and bioturbation features (root traces, coarse plant remains, mottling and mixed sediment textures) are common. Abundant gastropods and large millimetre to centimetre-size terrestrial plant remains.	**TIC** = 0·85 to 7·25% **TOC** = 1·00 to 5·85% **TN** = 0·10 to 0·50% **TOC/TN** = 6·2 to 22·70	Ephemeral saline lake–mud flat
	7 **Grey, banded to laminated carbonate-rich silts** Silt-sized particles of biogenic carbonates (*Chara* particles, gastropods) and minor amounts of quartz and plant remains included in a fine-grained matrix composed of authigenic carbonates (rice shaped and rhomboids) and phyllosilicates with gastropods and charophyte particles. Frequent intercalations of centimetre-thick grey coarser, sandy layers mainly composed of reworked biogenic carbonates.	**TIC** = 1·40 to 9·90% **TOC** = 0·44 to 2·80% **TN** = 0·03 to 0·16% **TOC/TN** = 5·11 to 38·3	Shallow, carbonate-producing lake

Table 4. (*Continued*)

Facies		Sedimentological features	Compositional parameters	Depositional subenvironment
Gypsum-rich facies	8	**Variegated, finely laminated gypsum, carbonates and clay** Decimetre-thick intervals composed of millimetre-thick white carbonate-rich laminae, yellowish gypsum-rich laminae and grey massive, clay-rich laminae. Frequent intercalations of brown, millimetre to centimetre-thick lacustrine organic-rich laminae and massive, centimetre-thick yellowish and light brown, massive coarse-grained silts organized in fining-upwards sequences composed of reworked gypsum and carbonate grains	**TIC** = 1·70 to 7·10% **TOC** = 0·45 to 2·40% **TN** = 0·06 to 0·18% **TOC/TN** = 6·9 to 23·15	Deep, saline, permanent lake with saline stratification
	9	**Variegated, banded gypsum, carbonates and clay** Sets of centimetre-thick alternating yellowish bands of gypsum with reworked biogenic carbonates, dark brown diatom ooze with lacustrine organic matter and lenticular gypsum and grey massive clays.	**TIC** = 0·10 to 7·15% **TOC** = 0 to 4·67% **TN** = 0·04 to 0·28% **TOC/TN** = 0 to 12·98	Deep saline lake
	10	**Yellowish, massive, coarse-grained gypsum** Millimetre to centimetre-thick rounded gypsum nodules embedded in a fine-grained silty matrix with lacustrine organic matter, reworked biogenic carbonates, 100 to 200 μm lenticular gypsum crystals and diatoms.	**TIC** = 0·38 to 2·60% **TOC** = 0 to 1·32% **TN** = 0·03 to 0·1% **TOC/TN** = 0 to 12·45	Ephemeral saline lake–mud flat

(B) Facies	Sedimentary sequence equivalent facies		Sedimentological features	Compositional parameters	Depositional subenvironment
Clastic facies	A	3	**Black, massive to laminated fine-grained silts**	**TIC** = 4 to 7·90% **TOC** = 3·90 to 6·50% **TN** = 0·50 to 0·8% **TOC/TN** = 7·40 to 8·30	Offshore, distal area
	B	2	**Dark grey massive silts with carbonates**	**TIC** = 4·15 to 7·85% **TOC** = 5·20 to 5·95% **TN** = 0·60 to 0·73% **TOC/TN** = 7·55 to 8·65	Transitional area
Carbonate-rich facies	C	7	**Banded to massive yellowish/light grey, carbonate-rich silts with plant remains and abundant bioturbation textures.**	**TIC** = 5·10 to 9·85% **TOC** = 1·30 to 7·75% **TN** = 0·15 to 0·70 **TOC/TN** = 7·9 to 11·5	Littoral platform

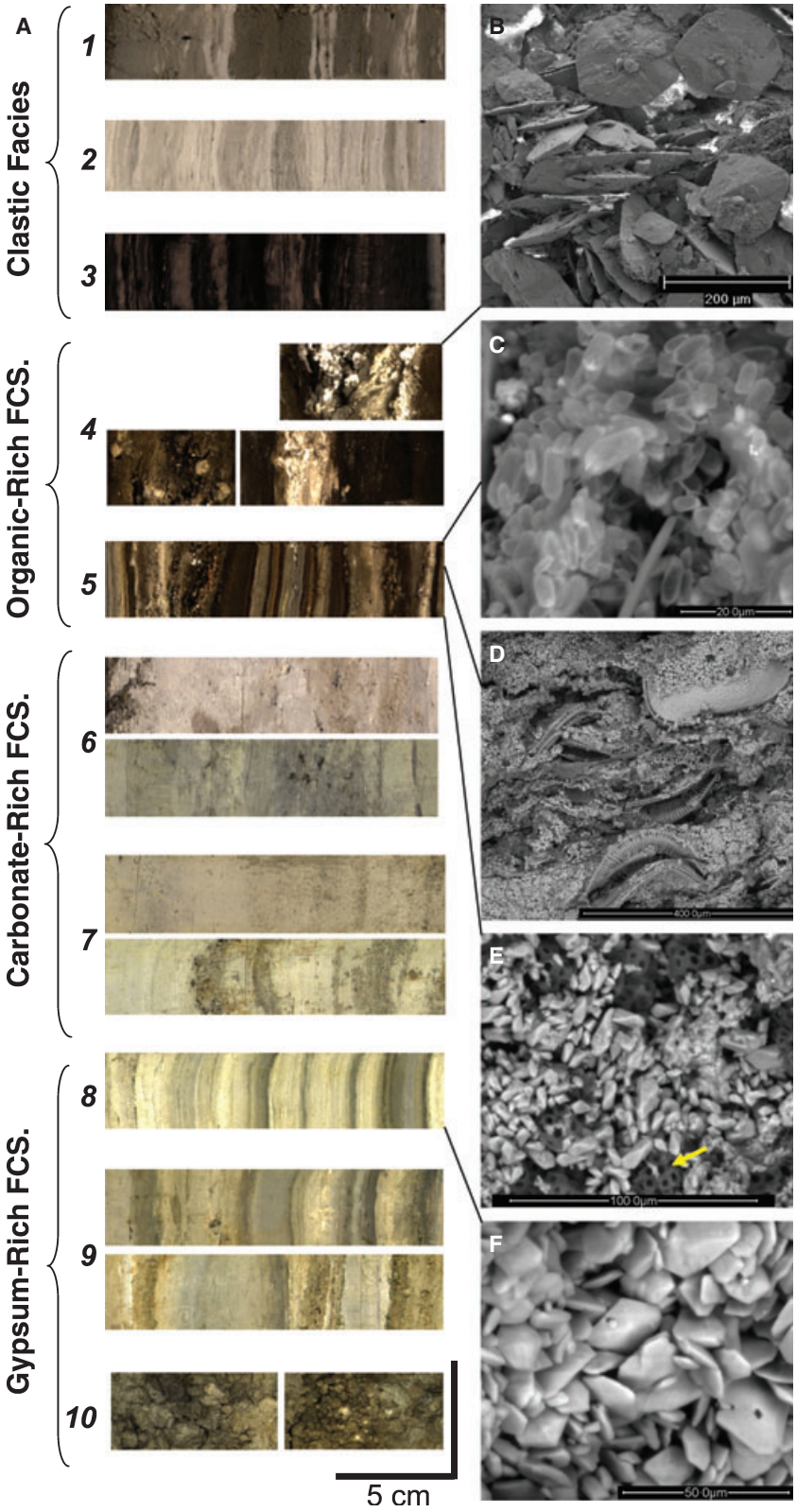

Fig. 6. (A) High-resolution core-scan images of sediment sections corresponding to the 10 different facies defined for the Lake Estanya sequence. (B) Secondary electron image; (C) to (F) Backscattered scanning electron images of sediment textures in selected intervals. (B) Lenticular gypsum crystals generated by intra-sedimentary growth up to 200 µm in size (in facies 4), (C) to (E) Facies 5. (C) Calcium carbonate crystals forming yellow laminae (in facies 5). (D) Gypsum crystals with *Botryococcus* colonies and diatoms in organic lamina. (E) Enlargement of prismatic gypsum crystals and *Botryococcus* (indicated by an arrow). (F) Lenticular (up to 25 µm long) gypsum crystals from facies 8.

and occasional macrophyte remains. These sediments are derived from the weathering and erosion of the soils and bedrock in the watershed and are transported to the lake. There are also minor amounts of endogenic material reworked from the littoral carbonate-producing environments.

The carbonate-rich facies occurs as banded to laminated decimetre-thick silt layers with massive, sandy intercalations. Sediments are composed mainly of calcite as well as minor amounts of quartz and clay minerals. Carbonates are biogenic grains (*Chara* fragments, micrite oncoids), carbonate coatings and small crystals derived either from direct precipitation in the epilimnion or from the reworking of particles produced in the littoral environments. Dolomite is less than 10% except in some massive and laminated facies (15 to 20% range).

The organic-rich facies occurs as finely laminated sediments in centimetre-thick to decimetre-thick layers composed of: (i) gypsum-rich sapropels with organic layers and gypsum laminae and nodules (Fig. 6A and B); and (ii) finely laminated, variegated intervals including several laminae types: microbial mats, organic ooze, carbonate (aragonite, calcite, HMC and dolomite), prismatic and nodular gypsum and occasionally clay (Fig. 6A, C, D and E).

The gypsum-rich facies is dominated by endogenic gypsum crystals or nodules. These nodules occur as: (i) finely laminated, variegated gypsum and carbonate mud layers; (ii) banded gypsum and carbonate mud layers; and (iii) irregular centimetre-thick nodular gypsum layers, mostly composed of accumulations of 300 μm lenticular gypsum crystals (Fig. 6A and F).

Riera *et al.* (2004) described a 1·57 m long sediment sequence retrieved in the sill between the two sub-basins in 1·5 m of water depth (Fig. 7). This sequence is composed of laminated carbonate facies alternating with massive reworked carbonate sands and gypsum-rich layers; they both are equivalent to the carbonate-rich and gypsum-rich facies, respectively, described in this facies model (Table 4). Analogously, the three main facies previously described for the present-day depositional sub-environments have their equivalents in the facies model (for details see Table 4B).

Core stratigraphy and chronology

The sedimentary sequence

Correlation between all the cores was based on lithology and magnetic susceptibility (Fig. 7). A composite sequence for Lake Estanya has been obtained using cores 1A and 5A (Fig. 8). Although the sediment–water interface was not preserved in core 1A, the upper part of the sequence was reconstructed using a short core correlated using OM and carbonate values (Morellón *et al.*, 2008). The upper 22 cm of the short core 0A were added to core 1A to complete the sequence (Fig. 9).

The Lake Estanya sequence has been divided into seven main sedimentary units and 28 sub-units, according to their sedimentary facies (Table 4A, Fig. 8). Correlation with the three main seismic units is shown in Figs 3 and 8.

Unit VII (957 to 775 cm core depth) corresponds to the lowermost part of seismic unit 'C'. It is composed of three main facies: carbonate-rich facies 7, gypsum-rich facies 9 and some clastic facies (facies 2.2).

Unit VI (775 to 630 cm) corresponds to the mid-part of seismic unit 'C' and is characterized by the deposition of variegated, finely laminated gypsum-rich facies 8 at the bottom and banded gypsum-carbonate facies 9 with centimetre-thick intercalations of clastic facies 2.2 at the top.

Unit V (630 to 536 cm) corresponds to the mid to upper part of seismic unit 'C'. The base of the unit is defined by a thick (25 cm) fining upward, carbonate facies 7 interval. The uppermost part of the sequence is characterized by alternating centimetre-thick layers of clastic facies 2.2 and gypsum-rich facies 9.

Unit IV (536 to 409 cm) corresponds to the uppermost part of seismic unit 'C' and it has been divided into two distinct intervals. The bottom part is characterized by alternating centimetre-thick bands of massive nodular gypsum facies 10 and carbonate, dolomite-rich facies 6; and the top section, where massive, carbonate–dolomite facies 6 are dominant.

Unit III (409 to 176 cm) corresponds to the lower and middle part of seismic unit 'B', and it is characterized by organic and gypsum facies 4 and 5 alternating with intercalations of banded clastic facies 2.1. The alternation of facies with the highest magnitude density changes is well-marked by the dense spacing of reflections of seismic unit 'B' (Fig. 3A).

Unit II (176 to 146 cm) comprises a lower facies 2.1 clastic-dominant sub-unit and an organic-rich interval with a centimetre-thick gypsum-rich sapropel intercalation (facies 4). This abrupt facies change has also been recorded by changes in the physical properties and as high-amplitude reflections in the seismic profiles.

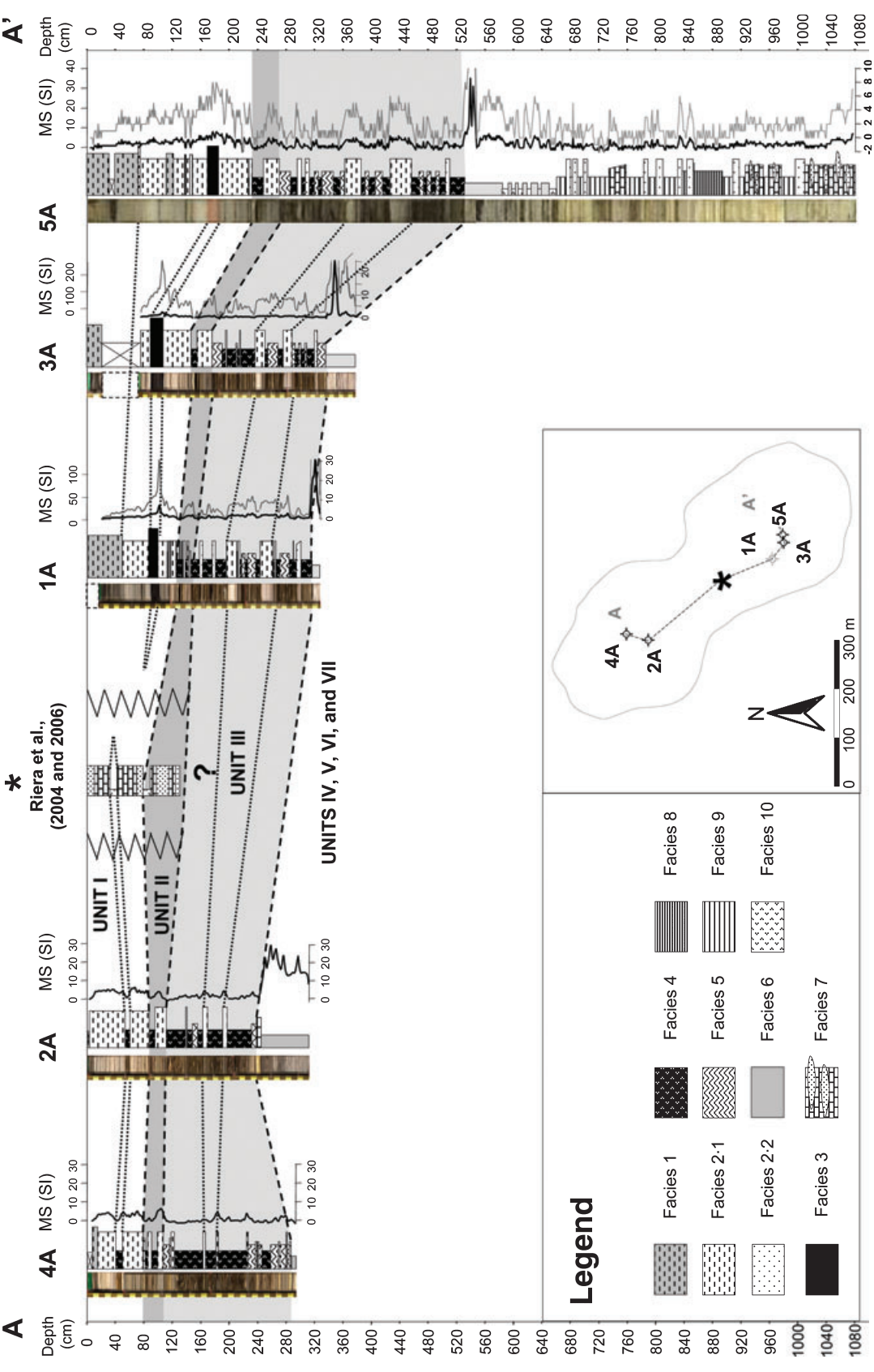

Fig. 7. Lithostratigraphic correlation panel of the five cores recovered in Lake Estanya Basin for this research (1A, 2A, 3A, 4A and 5A) and littoral core studied by Riera *et al.* (2004). Core images are accompanied by simplified sedimentological profiles and magnetic susceptibility (MS) core logs. In cores 1A, 3A and 5A, MS core logs are represented in two scales (thick black logs correspond to the upper scale, whereas grey logs correspond to the lower scale, in each case). Dashed horizontal lines represent correlation between main sedimentary units and dotted lines represent correlation between some sedimentary sub-units.

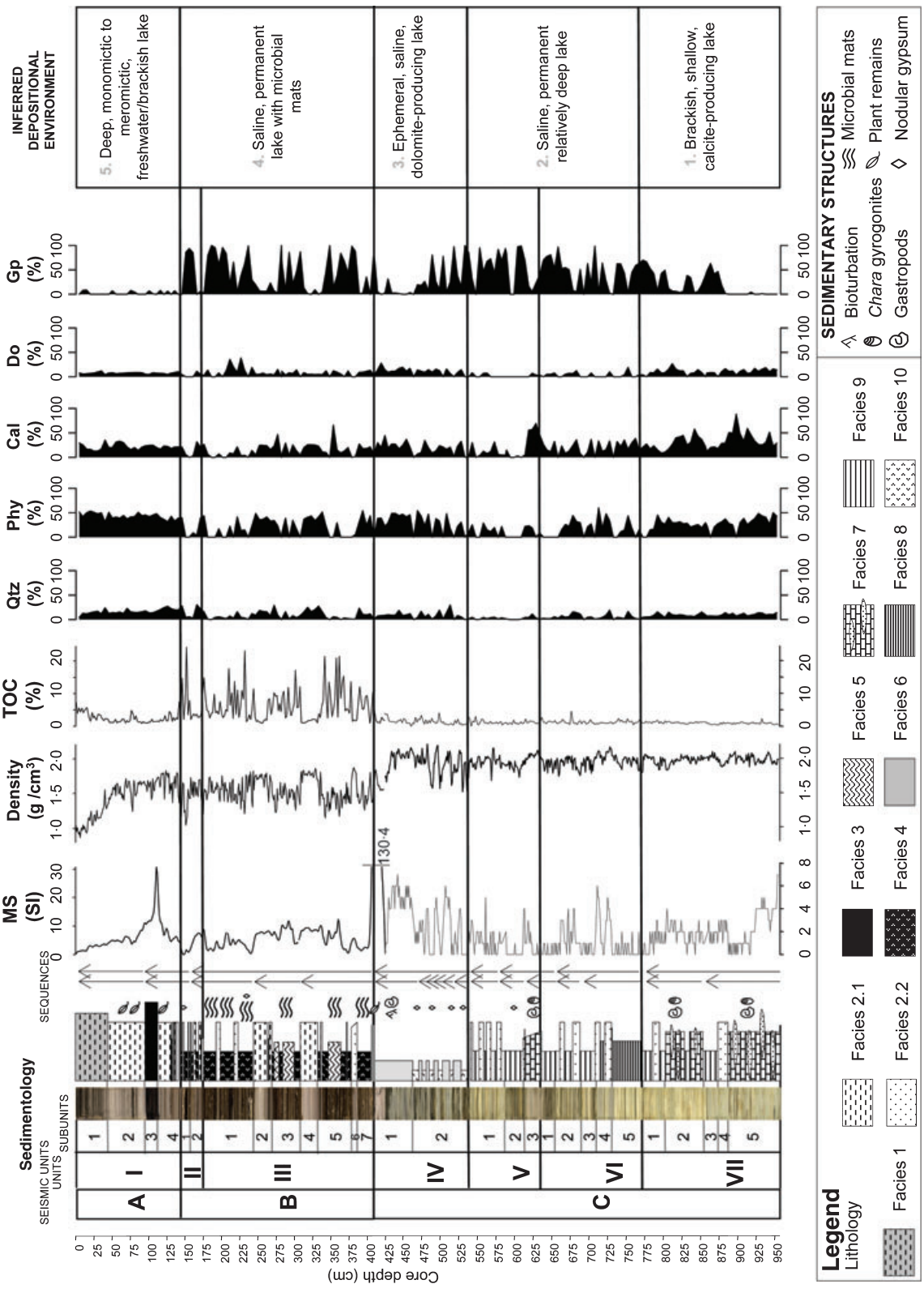

Fig. 8. Composite sequence of Lake Estanya sedimentary record formed by cores 1A and 5A. From left to right: seismic units, sedimentary units and sub-units, core images, sedimentological profile with sedimentary structures and interpreted sequences, magnetic susceptibility (MS) (SI units), density (g cc^{-1}), total organic carbon (TOC) (%), main mineralogical content (%), including quartz (Qtz), phyllosilicates (Phy), calcite (Ca), dolomite (Do) and gypsum (Gp) and the five inferred stages in the evolution of the lake basin. See legend below for facies and sedimentary structure symbols.

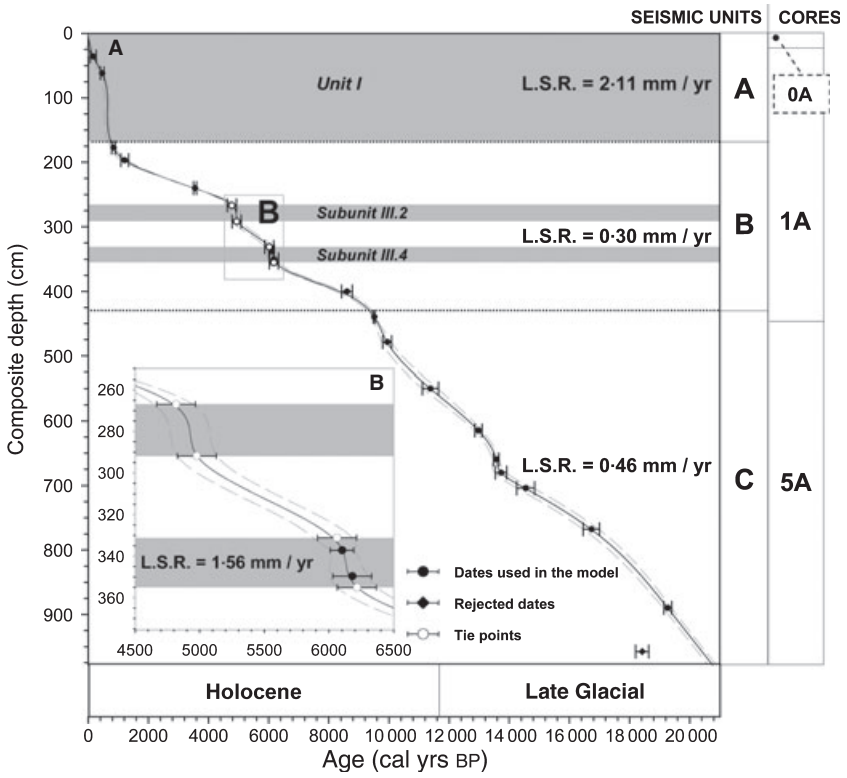

Fig. 9. (A) Chronological model of the composite sequence of Lake Estanya, formed by long cores 1A and 5A and short core 0A, based on mixed effect regression function (Heegaard *et al.*, 2005) of 17 accelerator mass spectrometry ^{14}C dates (black dots) and four tie points (white dots). A reversal date (diamond) is also represented (see legend at the bottom right). Continuous line represents the age–depth function framed by dashed lines (error lines). Horizontal dotted lines indicate seismic unit distribution with their corresponding linear sedimentation rates (LSR). Horizontal grey bands represent intervals characterized by clastic-dominant facies. (B) Detail of the four tie points calculated for clastic dominant intervals (sub-units III.2 and III.4) characterized by higher LSRs, inferred from radiocarbon dates analysed in sub-unit III.4.

Unit I (146 to 0 cm) overlies the mass-wasting deposit in the south-east sub-basin and it corresponds to seismic unit 'A', characterized by a lower density of reflections and predominant transparent seismic facies (Fig. 3A). The unit is composed of siliciclastic facies 1, 2.1 and 3. The base of the unit is composed of facies 2.1 with intercalation of millimetre-thick to centimetre-thick plant debris laminae. Intervals characterized by transparent seismic facies correspond to stable density values (lower half of the unit), whereas high amplitude reflections correspond to abrupt changes in the density values (top of the sequence) (Fig. 3A).

Age model

To construct the age model of the Estanya sequence, 17 radiocarbon dates from cores 1A and 5A (Table 3) were used. The reservoir effect is related to lake dynamics and is unlikely to remain constant through time. Unit I shows a similar depositional environment to recent lake conditions and, consequently, the same −585 ± 60 ^{14}C years reservoir effect has been applied. A reservoir effect correction of −820 ± 100 ^{14}C years was applied to bulk sediment samples corresponding to Units II to VI (Table 2). In Unit VIII, bulk OM age is 940 ± 170 years younger than a terrestrial organic macrorest at the same core depth, suggesting reworking from older deposits; both dates were rejected for the construction of the age model.

Linear sedimentation rates (LSR) obtained for clastic-dominant intervals ranging from 1·5 (sub-unit III.4) to 2 mm year^{-1} (Unit I) are much higher than those obtained for the rest of the sequence (0·2 to 0·5 mm year^{-1}) (Fig. 9A). Therefore, the LSR obtained from radiocarbon dates located within sub-unit III.4 was extrapolated for the rest of this sub-unit and also for sub-unit III.2, characterized by the same type of sedimentary facies. Thus, four tie points constraining the base and top of both clastic dominant intervals were obtained and introduced to improve the accuracy of the age model at these intervals (Fig. 9B).

Finally, the depth–age relationship for the sequence (Fig. 9A) was estimated by means of a generalized mixed-effect regression (Heegaard *et al.*, 2005) of 17 calibrated corrected dates (Table 3) and the four obtained tie points mentioned above. The average confidence interval of the error of the age model is *ca* 150 years. The resultant age–depth model for the Lake Estanya record described in this paper indicates that the *ca* 9·8 m of sediments spans from *ca* 21 cal kyr BP to the present.

DISCUSSION

Depositional history and sedimentary environments during the last 21 kyr

Based on seismic stratigraphy and facies associations (Table 3), five main stages can be inferred for the evolution of Lake Estanya during the last 21 kyr (Fig. 10).

Stage 1: A shallow, carbonate-producing lake during the Last Glacial Maximum (21 to 17·3 kyr BP)

The karstification processes and collapse that created the two sinkholes occurred more than 20 kyr ago, prior to the deposition of Unit VII. The seismic survey shows that, during this early stage, deposition was restricted to the central areas of both sub-basins that remained predominantly disconnected until the onset of the Holocene (Fig. 3A). The oldest sediments recovered (Unit VII) indicate a relatively shallow carbonate-producing lake system during the Last Glacial Maximum, characterized by deposition of grey, banded to faintly laminated carbonate silts with centimetre-thick sandy lenses (facies 7).

This facies formed in a relatively shallow setting, characterized by the presence of submerged macrophytes and aquatic plants and intense bioturbation in oxic bottom conditions. *Chara* sp. was the main producer of biogenic carbonate particles further reworked by wave action. External clastic input was limited, which may be due to the combination of the presence of a littoral vegetation belt and reduced run-off (Fig. 10).

Similar environments occur in modern littoral zones (facies A) and in the shallow sill areas (facies S1 and S2, Riera *et al.*, 2004). Littoral environments with high carbonate productivity occur in many karstic lakes in the Iberian Peninsula: La Cruz (Romero *et al.*, 2006; Romero-Viana *et al.*, 2008), carbonate-rich wetlands associated with fluvial settings, e.g. Tablas de Daimiel (Álvarez Cobelas & Cirujano, 1996; Domínguez-Castro *et al.*, 2006) or tufa-dammed lakes, as Ruidera (Ordóñez *et al.*, 2005) and Taravilla (Valero Garces *et al.*, 2008). More examples of these depositional environments can be found elsewhere in the Mediterranean basin, as Lake Vrana (Schmidt *et al.*, 2000) and in many 'marl' lakes (Murphy & Wilkinson, 1980; Platt & Wright, 1991).

Fluctuations in lake level and water chemical concentration led to deposition of carbonate (facies 7) and gypsum (facies 9) sequences. Although there is no clear evidence of increased subsidence as a result of karstic processes at this time, the presence of freshwater carbonates could be interpreted as evidence of an early stage of karstic lake development, when the hydrological system was relatively open because the bottom of the lake was not completely sealed off. A short residence time for lake water, as a result of a connection with the aquifer during periods of increased subsidence, could explain the absence of evaporite facies at the base of the sequence. Alternatively, the presence of freshwater carbonates could imply a more positive water balance.

Stage 2: A permanent, relatively deep saline lake during the late glacial (17·3 to 11·6 kyr BP)

The occurrence of finely laminated gypsum-rich facies 8 along Units V, VI and VII marks the development of a stratified, saline and relatively deep lake lasting for some millennia. Facies 8 represents primary gypsum deposition (cumulate crystals) in distal areas of a relatively deep saline lake, in which banded carbonate and gypsum silt (facies 9) and clastic facies 2.2 are deposited in the more littoral areas (Fig. 10). Laminae preservation suggests anoxic environments. Anoxic conditions at the bottom of the lake could have resulted from water stratification induced by a higher salinity in the hypolimnion as found in some lakes in the northern Great Plains (Valero-Garcés & Kelts, 1995; Last & Vance, 1997), where gypsum laminae are also formed.

The development of such a system suggests that the lake basin had been plugged by sediments and leaks to the aquifers became minimal (mature stage) leading to evaporite formation. A progressive regression trend occurred and distal finely laminated facies 8 were gradually replaced by cycles of clastic facies 2.2 (flooding) and gypsum facies 9 (desiccation). At about 13·5 kyr BP, deposition of carbonate-rich facies 7 indicates a brief return towards freshwater to brackish conditions. A shallow saline lake developed afterwards characterized by alternating gypsum-rich facies 9 and centimetre-thick intercalations of massive clastic inputs, represented by facies 2.2.

Stage 3: A shallow saline lake–saline mudflat during the transition to the Holocene (from 11·6 ka to 9·4 kyr BP).

During this period, represented by the deposition of Unit IV, Lake Estanya was a shallow, ephemeral, saline lake–mud flat with carbonate-

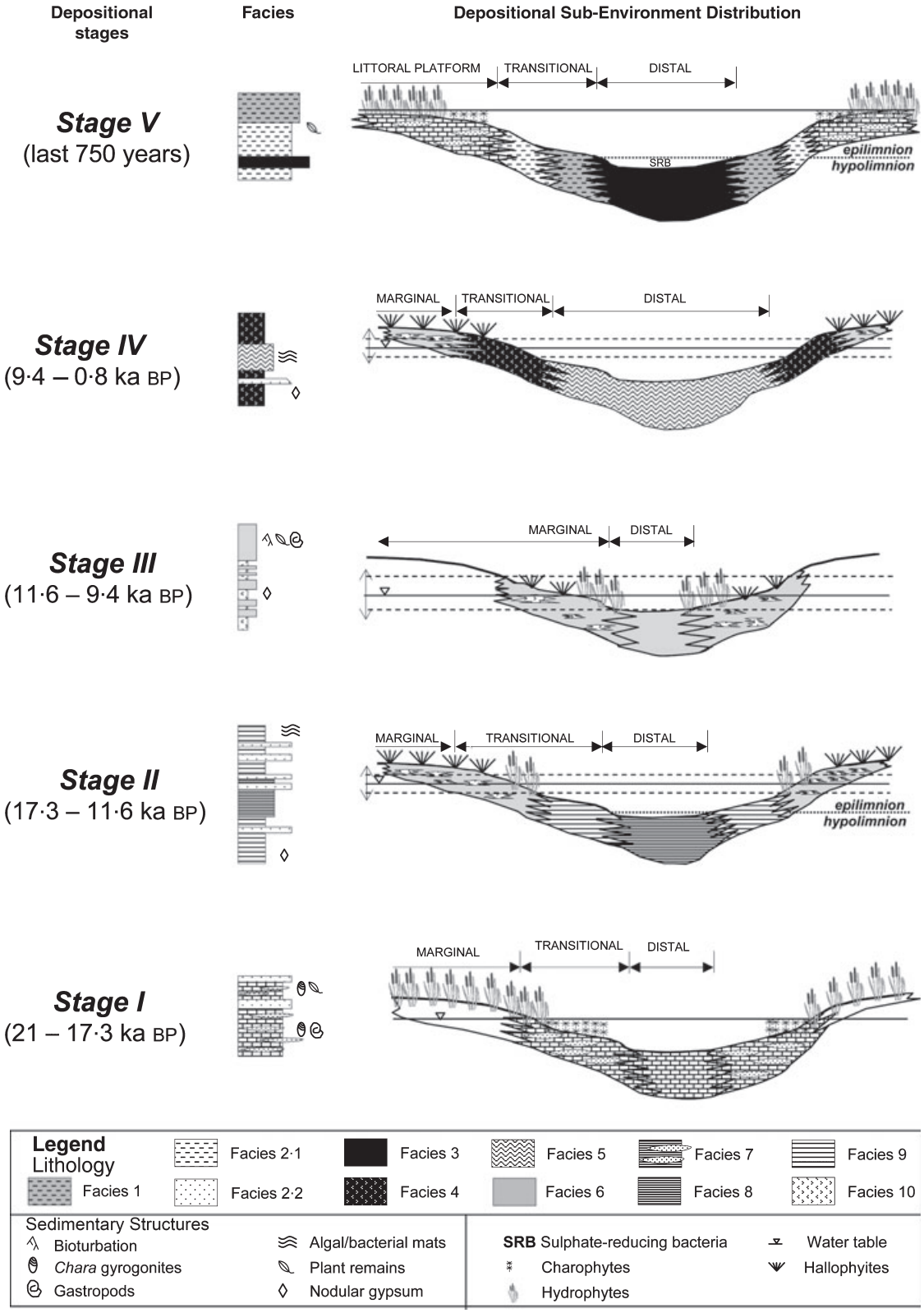

Fig. 10. Facies model sketches showing the main depositional environments interpreted for the five main stages identified in the evolution of the Lake Estanya sedimentary record. From bottom to top: Stage I (shallow, carbonate-producing lake); Stage II (permanent, relatively deep, saline lake); Stage III (shallow saline lake–saline mud flat); Stage IV (saline lake with microbial mats); and Stage V (brackish to freshwater, deep lake). For each depositional environment, deposition time-period, facies sequences and depositional sub-environments spatial distribution are also indicated (see legend below).

dominated sedimentation during flooding episodes (facies 6) and gypsum precipitation as nodules and large intrasediment crystals (facies 10) during desiccation phases. The occurrence of interstitial and intra-sedimentary gypsum crystals and the presence of dolomite are characteristic of dominant shallow conditions with frequent periods of subaerial exposure and evaporite pumping processes (Last, 1990). The increase in magnetic susceptibility values and the sharp peak at the top of the unit reflect both an increase in clastic input and the occurrence of oxidation processes coherent with frequent subaerial conditions (Morellón *et al.*, 2008).

Examples of this depositional environment can be found in marginal playa lake settings characterized by the deposition of alternating carbonate and gypsum-rich interstitial facies (Schreiber & Tabakh, 2000). Modern analogues occur at nearby sites in the Central Ebro Basin saline lakes, e.g. La Playa (Valero-Garcés *et al.*, 2004); Gallocanta (Pérez *et al.*, 2002; Rodó *et al.*, 2002; Corzo *et al.*, 2005); Lake Chiprana (Valero-Garcés *et al.*, 2000); as well as in other areas of the Iberian Peninsula (Reed, 1998) and the Mediterranean basin (Schreiber & Tabakh, 2000).

Stage 4: A saline lake with abundant microbial mats during the Holocene (9·4 to 0·8 kyr BP)

The deposition of seismic unit 'B' marks a general increase in lake level, leading to the connection of the two sub-basins. Sedimentary Unit III started with deposition of a coarse clastic layer with large plant debris, deposited throughout the lake basin reflecting a flood episode, responsible for the increase of lake level and the establishment of a relatively deep saline lake.

Two facies are dominant during this stage: (i) massive organic ooze with nodular and lenticular gypsum interpreted as deposition in the marginal zones, affected by strong fluctuations in lake level and seasonal desiccation (facies 4); and (ii) variegated, laminated facies 5 interpreted as deposition in the intermediate and distal zones, with more stable lake levels, relatively deep, but with enough light reaching the lake bottom to allow the development of microbial mats. Frequent anoxic conditions and saline stratification were conducive to aragonite and gypsum formation and laminae preservation (Valero-Garcés & Kelts, 1995).

Shallow saline lake systems, such as that interpreted for stage 4, are affected strongly by fluctuations in lake level, and littoral areas are affected by frequent seasonal desiccation periods (Last, 1990; Schreiber & Tabakh, 2000). The occurrence of microbial mats is common in these shallow saline systems (Bauld, 1981). The substantial development of benthonic microbial mats with aragonite laminae as distal facies 5 indicates a higher organic productivity than during late glacial times and limits the maximum depositional water depth to a few metres where light can still reach the lake bottom. Thin clastic intercalations (facies 2.2) such as in sub-unit III.6 mark flood events reaching the centre of the lake, whereas thicker intervals of carbonate–siliciclastic facies 2.1, represented by sub-units III.2 and III.4, are interpreted as being deposited during longer periods of increased runoff, occurring during the early and mid-Holocene.

Saline conditions were dominant again after 4·8 kyr BP, as indicated by the deposition of gypsum-rich facies 10 and massive sapropels facies 4 (sub-unit III.1); terrigenous input from the catchment was restricted to centimetre-thick clastic intercalations. The abundance of gypsum nodules and the decrease in carbonate content indicate that more saline conditions and shallower lake levels lasted until 1·2 kyr BP. Although major changes in sedimentation appear to be synchronous throughout the basin and main units can be easily correlated (Fig. 7), significant lateral facies changes between the two sub-basins occur through Unit III. More proximal facies occur in the north-west sub-basin, where clastic facies are reduced and massive gypsum-rich sapropels (facies 4) are dominant over microbial mats (facies 5) during this period (Fig. 7).

A transition towards less saline conditions, higher lake level and increased runoff is represented by the deposition of Unit II (1200 to 870 cal yr BP). This transgressive period was interrupted by the deposition of a thick gypsum layer (Unit II.1), indicating a sharp drop in lake level and more saline conditions around 750 cal yr BP, according to the age model used here. Similar depositional environments can be found in transitional to distal areas of playa lake settings, as indicated in examples listed previously for stage 4.

Stage 5: A brackish to freshwater, deep lake since the 12th Century (750 cal yr BP to present)

The abrupt lake level drop at 750 cal yr BP marked by the deposition of Unit II coincided with the emplacement of the mass-wasting unit 'D'. This

deposit is overlain by a thick clastic sequence (Unit I) continuously deposited throughout the whole lake basin as indicated by seismic data. The absence of gypsum deposition and the dominance of fine-grained clastic sedimentation (clastic facies 1, 2 and 3) indicate lower salinity, generally higher lake level and an increase in sediment delivery to the lake. Higher clastic input probably is related to the development of agriculture in the area during medieval times (Riera *et al.*, 2004).

Facies and depositional sub-environments are similar to the present-day distribution. The lake has considerable water depth and frequent seasonal or permanent anoxic lake bottom conditions. Clastic input from the watershed is high, and carbonate production is restricted to the epilimnion and to the littoral areas where it is the dominant depositional process. Three main facies associations and sub-environments can be identified: (i) littoral platform; (ii) transitional area; and (iii) distal area (Figs 5 and 10). Littoral and transitional facies would correspond to those described by Riera *et al.* (2004) in the core from the sill between the two sub-basins (facies S1 and S2), and facies A and B identified in the modern lake survey, all of them corresponding to core facies 7.

Modern analogue systems to this depositional environment in the Iberian Peninsula are Lake Banyoles (Julià, 1980); Lake Montcortés (Camps *et al.*, 1976; Miracle & Gonzalvo, 1979; Modamio *et al.*, 1988); and Lake Zoñar (Valero-Garcés *et al.*, 2006). Many deep lakes in the karstic regions of the Mediterranean correspond to this depositional setting [e.g. Lake Salda, Turkey (Kazanci *et al.*, 2004); Lake Vrana, Croatia (Schmidt *et al.*, 2000)].

Although lake level remained relatively high during this stage, significant hydrological fluctuations occurred. Deposition of facies 1, characterized by a black colour and high magnetic susceptibility values, as a consequence of sulphide formation under permanent anoxic hypolimnetic conditions (Morellón *et al.*, 2008), probably represents the deepest lake level conditions recorded throughout the sequence. Deposition of this unit is restricted to the deepest south-east basin, indicating that this long-term water stratification only affected the deepest areas of the lake (Fig. 7). Finally, the deposition of sub-units 1 and 2 indicate a shallower sub-environment characterized by a return towards the monomictic, seasonal water stratification prevailing today in Lake Estanya.

Factors controlling sedimentation in Lake Estanya

The interpretation of the sedimentary sequence and the basin architecture of Lake Estanya allowed the definition of a depositional model characterized by a large variability of facies and depositional sub-environments during the last 21 kyr. Most factors affecting sedimentation in lakes responded to internal thresholds, leading to abrupt lateral and vertical changes in facies (Valero-Garcés & Kelts, 1995). Although most of these changes respond to feedback mechanisms, and they are all inter-related, they are governed directly or indirectly by fluctuations in lake level and, consequently, the evolution of the basin is greatly controlled by the hydrology. However, the occurrence of extreme events (floods, mass-wasting processes) and changes in the watershed (land use) can also affect the lake dynamics and sedimentation patterns. The main factors controlling sedimentation in Lake Estanya are: (i) karstic processes; (ii) hydrology; (iii) water salinity; (iv) water stratification; (v) clastic input; and (vi) mass-wasting processes.

(i) *Karstic processes* (collapse, subsidence and dissolution) were responsible for the formation of the basin and the functioning of the hydrogeological system. Initial lake formation is related directly to the karst topography of the bedrock and mechanical and dissolution processes that generate the accommodation space for the lake (Kindinger *et al.*, 1999; Gutiérrez *et al.*, 2008). Lateral continuity of the seismic reflections in the northern sub-basin indicates that there was no significant subsidence during the last 20 kyr. Seismic stratigraphy in the southern sub-basin is more complex and characterized by strong sediment thickness variations and by an irregularly shaped acoustic basement probably suggesting some collapse activity during the early late glacial stage, when the lower part of unit 'C' was deposited (transitional phase). Modern Lake Estanya fits the category of a mature, base-level phase karst lake, according to the Kindinger *et al.* (1999) classification.

(ii) *The hydrological balance and lake-level fluctuations* are the main factors controlling facies distribution and composition. In Lake Estanya, there is no evidence of significant changes in the hydrogeological behaviour of the lake system because the basin became sealed-off during the late glacial. It is assumed that increased rainfall would have caused increased groundwater and spring flow in the past.

(iii) *Water salinity and chemical composition* generally varies inversely with water level, as a result of the hydrological balance (Street-Perrott & Harrison, 1985). In Lake Estanya, salinity changes have controlled the precipitation of different carbonate and sulphate phases and the development of different biota adapted to particular conditions. The recycling of previously deposited salts during saline stages, however, had a strong impact on the chemical composition of lake waters and may have led to decoupling of lake water volume and chemical concentration.

(iv) *Water stratification* can be achieved in karstic lakes through thermal processes and by large chemical gradients. The development of seasonal or permanent thermal stratification requires a minimum water depth of 6 m (Shaw *et al.*, 2002). Thermal stratification is dominant in present-day Lake Estanya and seems to have also been prevalent during the last 800 years. Lake depth is the main parameter currently controlling thermal stratification. At this time, permanent anoxic conditions only developed in the deeper southern basin leading to deposition of facies 3. In the northern, shallower sub-basin, only seasonal stratification occurred.

However, in the past, chemical processes have played a major role in water stratification during both high-lake and low-lake periods. In saline lakes, meromictic conditions can occur when a large gradient between denser, chemically concentrated waters in the hypolimnion and fresher waters in the epilimnion is established. There are numerous examples of relatively deep, meromictic lakes with laminated salt deposition in the hypolimnion, as stated above. A setting of this type is interpreted for deposition of the laminated gypsum-rich facies 8 in Unit VI. Because of a high chemical concentration, some shallow saline lakes could also become stratified and anoxic at the bottom; this would be the case for Lake Estanya during some depositional intervals of Unit III.

(v) *Clastic input* mainly depends on external parameters, such as the availability of sediments in the catchment area, climatic conditions, topography, vegetation cover, land uses, presence of littoral vegetation and aquatic macrophytes acting as a barrier to sediment delivery. Extreme flood events occurred during the last 20 kyr and their sedimentological signature (facies 2.2) is found in the distal facies of all depositional environments; fresh, saline, deep and shallow. However, higher general clastic input into the lake only occurs in the upper part of Unit I and in sub-units III.2 and II.4. The mid-Holocene episodes probably are associated with periods of higher precipitation and runoff. However, the abrupt change in lake dynamics during the last 800 years probably is a reflection of anthropogenic impact in the watershed.

(vi) *Mass-wasting processes* are a common feature in lake basins with steep margins (Chapron *et al.*, 2004; Girardclos *et al.*, 2007; Strasser *et al.*, 2007). Initial local, subaqueous slope instabilities are generated when the shear stress in the sediments can no longer sustain the gravitational downslope forces (Coleman & Prior, 1988; Hampton *et al.*, 1996). The largest mass-wasting deposit identified in the Lake Estanya basin is restricted to the south-east sub-basin and emplaced prior to the deposition of Unit I. Both the external structure, characterized by a wedge shape with a lobe-shaped distal termination and an irregular lower and upper surface (hummocky), and the internal structure (transparent to chaotic seismic facies), indicates the loss of internal structure typical of a mass flow (Schnellmann *et al.*, 2005). This mass-flow deposit occurred during a transgressive phase leading to higher lake levels and during a period of increased sediment delivery to the lake. There are many factors responsible for slope instabilities in lakes: earthquakes (Schilts & Clague, 1992), sediment overloading, rapid water level changes, cyclic loading by waves and biogenic gas production from the decay of OM (Nisbet & Piper, 1998). Although the abrupt transition from low-lake level and gypsum deposition (Unit II) to higher-lake level and clastic deposition (Unit I) might have played a role in the generation of this deposit, none of the other factors can be ruled out. Earthquakes in this sector of the Pyrenean Range have been reported during the Holocene (Alasset & Meghraoui, 2005; Gutierrez-Santolalla *et al.*, 2005). In particular, the east-west trending North Maladeta Fault has been identified as the most probable source of the Ribagorza earthquake of 1373 AD (Olivera *et al.*, 1994, 2006), with an estimated magnitude of M_W 6·2. Additionally, a major change in land-use occurred during mediaeval times (Riera *et al.*, 2004, 2006). It is hypothesized that a higher sediment load to the lake due to increased farming practices during higher-lake levels created the conditions conducive to mass-wasting episodes. Seismic activity (the Ribagorza earthquake) could have triggered these events.

CONCLUSIONS

The spatial distribution of sedimentary facies in Lake Estanya allows the identification of three main depositional sub-environments: (i) the littoral carbonate-producing platform; (ii) the transitional, steep talus; and (iii) the offshore, distal area. The distribution of these sub-environments is conditioned strongly by lake bathymetry which today exerts a key influence on the depositional conditions.

As in most small relatively deep karstic lakes, the main factors controlling sedimentation are: hydrological balance and lake-level changes, water salinity and chemical composition, water stratification, clastic input and the occasional occurrence of mass-wasting and karstic activity. The interplay of these processes during the depositional history results in a complex vertical and lateral alternation of 10 different sedimentary facies, indicative of five different depositional environments. A brackish, shallow, calcite-producing lake was established during the full glacial period, probably after a period of increased karstic (solution and collapse) activity that created more accommodation space in the basin. When the lake basin was sealed-off completely, a permanent, saline, relatively deep lake developed during the late glacial. A shallow, brackish to saline, ephemeral, dolomite-producing lake occurred during the transition to the Holocene and was substituted by a saline shallow lake with microbial mats, lasting from the early to the late Holocene. Finally, changes in land use of the watershed and a rise in lake level induced a large increase in sediment input to the lake. Thus, a freshwater to brackish, permanent, deep meromictic to monomictic lake, similar to the present-day conditions, remained during the last 800 years.

The sedimentary facies model defined for Lake Estanya, integrated with seismic stratigraphy, provided a detailed reconstruction of the depositional history of the basin showing abrupt and large hydrological changes during the last 21 kyr. Further research will clarify the timing and extent and of the environmental changes which are archived in this lake sequence.

ACKNOWLEDGEMENTS

Financial support for research was provided by the Spanish Inter-Ministry Commission of Science and Technology (CICYT), through the projects LIMNOCLIBER (REN2003-09130-C02-02), IBERLIMNO (CGL2005-20236-E/CLI), LIMNO CAL (CGL2006-13327-C04-01) and GRACCIE (CSD2007-00067). Additional funding was provided by the Instituto de Estudios Altoaragoneses (IEA). The Aragonese Regional Government – CAJA INMACULADA partially funded XRD analyses, seismic studies and XRF analyses at University of Cádiz, ETH-Zurich, University of Geneva and MARUM Centre (University of Bremen), respectively, by means of two travel grants.

M. Morellón is supported by a PhD contract with the CONAI+D (Aragonese Scientific Council for Research and Development), A. Moreno holds a ESF – Marie Curie programme post-doctoral contract, M. Rico holds a 'Juan de la Cierva' contract from the Spanish Government and J. P. Corella holds a CONAI+D PhD fellowship. We are indebted to Anders Noren, Doug Schnurrenberger and Mark Shapley (LRC-University of Minnesota) for the 2004 coring campaign and Santiago Giralt and Armand Hernández (IJA-CSIC), as well as Alberto Sáez and J.J. Pueyo-Mur (University of Barcelona) for coring assistance in 2006. We are also grateful to ETH-Zürich, University of Geneva, MARUM Centre (University of Bremen), IGME, EEAD-CSIC and IPE-CSIC laboratory staff for their collaboration in this research. We thank anonymous reviewers and Associate Editor, Stephen Lokier, for their helpful comments and their criticism, which led to a considerable improvement of the manuscript.

REFERENCES

Alagöz, C.A. (1967) *Sivas Çevresi ve Doğusunda Jips Karstı Olaylarıı-Les phénomènes karstiques du gypse aux environs et à l'est de Sivas*. Ankara Üniversitesi Dil ve Tarih-Coğrafya Fakültesi Yayımıı, Ankara, 126 pp.

Alasset, P.-J. and **Meghraoui, M.** (2005) Active faulting in the western Pyrenees (France): paleoseismic evidence for late Holocene ruptures. *Tectonophysics*, **409,** 39–54.

Álvarez Cobelas, M. and **Cirujano, S.** (1996) *Las Tablas de Daimiel*. Ecología acuática y sociedad, Madrid, 23–29 pp.

Anselmetti, F.S., Ariztegui, D., Hodell, D.A., Hillesheim, M.B., Brenner, M., Gilli, A., McKenzie, J.A. and **Mueller, A.D.** (2006) Late Quaternary climate-induced lake level variations in Lake Peten Itza, Guatemala, inferred from seismic stratigraphic analysis. *Palaeogeogr. Palaeoclimatol. Palaeoecol.*, **230,** 52–69.

Ávila, A., Burrel, J.L., Domingo, A., Fernández, E., Godall, J. and **Llopart, J.M.** (1984) Limnología del Lago Grande de Estanya (Huesca). *Oecologia Aquatica*, **7,** 3–24.

Balch, D.P., Cohen, A.S., Schnurrenberger, D.W., Haskell, B.J., Valero Garces, B.L., Beck, J.W., Cheng, H. and **Edwards, R.L.** (2005) Ecosystem and paleohydrological response to Quaternary climate change in the Bonneville Basin, Utah. *Palaeogeogr. Palaeoclimatol. Palaeoecol.*, **221,** 99–122.

Bauld, J. (1981) Occurrence of benthic microbial mats in saline lakes. *Hydrobiologia*, **81–82,** 87–111.

Bohacks, K.M., Carroll, A.R., Neal, J.E. and **Mankiewicz, P.J.** (2000) Lake-basin type, source potential, and hydrocarbon character: an integrated-sequence-stratigraphic-geochemical framework. In: *Lake Basins Through Space and Time* (Eds E.H. Gierlowski-Kordesch and K.R. Kelts), *AAPG Stud. Geol.*, **46,** 3–34.

Bourrouilh-Le Jan, F.G., Beck, C. and **Gorsline, D.S.** (2007) Catastrophic events (hurricanes, tsunami and others) and their sedimentary records: introductory notes and new concepts for shallow water deposits. *Sed. Geol.*, **199,** 1–11.

Brown, E.T., Johnson, T.C., Scholz, C.A., Cohen, A.S. and **King, J.W.** (2007) Abrupt change in tropical African climate linked to the bipolar seesaw over the past 55 000 years. *Geophys. Res. Lett.* **34,** doi: 10.1029/2007GL031240.

Buurman, P., Pape, T. and **Muggler, C.C.** (1997) Laser grain-size determination in soil genetic studies: I. *Practical problems. Soil Science*, **162,** 211–218.

Camps, J., Gonzalvo, I., Güell, J., López, P., Tejero, A., Toldrà, X., Vallespinos, F. and **Vicens, M.** (1976) El lago de Montcortès, descripción de un ciclo anual. *Oecologia Aquatica*, **2,** 99–110.

Chapron, E., Van Rensbergen, P., De Batist, M., Beck, C. and **Henriet, J.P.** (2004) Fluid-escape features as a precursor of a large sub-lacustrine sediment slide in Lake Le Bourget, NW Alps, France. *Terra Nova*, **16,** 305–311.

Chung, F.H. (1974a) Quantitative interpretation of X-ray diffraction patterns of mixtures. I. Matrix-flushing method for quantitative multicomponent analysis. *J. Appl. Crystallogr.*, **7,** 000.

Chung, F.H. (1974b) Quantitative interpretation of X-ray diffraction patterns of mixtures. II. Adiabatic principle of X-ray diffraction analysis of mixtures. *J. Appl. Crystallogr.*, **7,** 526–531.

Cohen, A.S. (2003) *Paleolimnology: The History and Evolution of Lake Systems*. Oxford University Press, New York, 500 pp.

Coleman, J.M. and **Prior, D.B.** (1988) Mass wasting on continental margins. *Annu. Rev. Earth Planet. Sci.*, **16,** 101–119.

Corzo, A., García de Lomas, J., Van Bergeijk, A., Luzón, A., Mayayo, M.J. and **Mata, P.** (2005) Carbonate mineralogy along a biogeochemical gradient in recent lacustrine sediments of Gallocanta Lake (Spain). *Geomicrobiol. J.*, **22,** 1–16.

Cvijic, J. (1981) The dolines: translation of geography. In: *Karst Geomorphology* (Ed. M.M. Sweeting), pp. 225–276. Hutchinson, Pennsylvania.

Dean, W.E. (1981) Carbonate minerals and organic matter in sediments of modem north-temperate hard-water lakes. in: *Recent and Ancient Nonmarine Depositional Environments: Models for Exploration* (Eds E.G. Ethridge and R.M. Flores), *SEPM Spec. Publ.*, **31,** 213–231.

Dean, W.E. and **Fouch, T.D.** (1983) Lacustrine environment. In: *Carbonate Depositional Environments* (Eds R.A. Schole, D.G. Bebout and C.H. Moore), *AAPG Mem.*, **33,** 96–130.

Domínguez-Castro, F., Santisteban, J.I., Mediavilla, R., Dean, W.E., López-Pamo, E., Gil-García, M.J. and **Ruiz-Zapata, M.B.** (2006) Environmental and geochemical record of human-induced changes in C storage during the last millennium in a temperate wetland (Las Tablas de Daimiel National Park, central Spain). *Tellus B*, **58,** 573–585.

Esteve, I., Guerrero, R., Montesinos, E. and **Abellà, C.** (1983) Electron microscope study of the interaction of epibiontic bacteria with Chromatium minus in natural habitats. *Microbial Ecol.*, **9,** 57–64.

Eugster, H.P. and **Hardie, L.A.** (1978) Saline lakes. In: *Lakes, Chemistry, Geology, Physics* (Ed. A. Lerman), pp. 237–293. Springer, New York.

Eugster, H.P. and **Kelts, K.R.** (1983) Lacustrine chemical sediments. In: *Chemical Sediments and Geomorphology* (Eds A.S. Goudie and K. Pye), pp. 321–368. Academic Press, London.

Fritz, S.C., Baker, P.A., Seltzer, G.O., Ballantyne, A., Tapia, P., Cheng, H. and **Edwards, R.L.** (2007) Quaternary glaciation and hydrologic variation in the South American tropics as reconstructed from the Lake Titicaca drilling project. *Quatern. Res.*, **68,** 410–420.

Gierlowski-Kordesch, E.H. and **Kelts, K.R.** (1994) *Global Geological Record of Lake Basins*. Cambridge University Press, Cambridge, 427 pp.

Gierlowski-Kordesch, E.H. and **Kelts, K.R.** (2000) *Lake Basins Through Space and Time*. The American Association of Petroleum Geologists, Tulsa, OK, 648 pp.

Girardclos, S., Schmidt, O.T., Sturm, M., Ariztegui, D., Pugin, A. and **Anselmetti, F.S.** (2007) The 1996 AD delta collapse and large turbidite in Lake Brienz. *Mar. Geol.*, **241,** 137–154.

Guerrero, R., Pedrós-Alió, C., Esteve, I. and **Mas, J.** (1987) Communities of phototrophic sulfur bacteria in lakes of the Spanish Mediterranean region. *Acta Academiae Aboensis*, **2,** 125–151.

Gutiérrez, F., Calaforra, J., Cardona, F., Ortí, F., Durán, J. and **Garay, P.** (2008) Geological and environmental implications of the evaporite karst in Spain. *Environ. Geol.*, **53,** 951–965.

Gutiérrez-Elorza, M. (2001) *Geomorfología Climática*. Editorial Omega, Barcelona, 642 pp.

Gutierrez-Santolalla, F., Acosta, E., Rios, S., Guerrero, J. and **Lucha, P.** (2005) Geomorphology and geochronology of sackung features (uphill-facing scarps) in the Central Spanish Pyrenees. *Geomorphology*, **69,** 298–314.

Hampton, M.A., Lee, H.J. and **Locat, J.** (1996) Submarine landslides. *Rev. Geophys.* **34,** 33–59.

Hardie, L.A., Smoot, J.P. and **Eugster, H.P.** (1978) Saline lakes and their deposits: a sedimentological approach. In: *Modern and Ancient Lake Sediments* (Eds A. Matter and M.E. Tucker), *Int. Assoc. Sedimentol. Spec. Publ.*, **2,** 7–42.

Heegaard, E., Birks, H.J.B. and **Telford, R.J.** (2005) Relationships between calibrated ages and depth in stratigraphical sequences: an estimation procedure by mixed-effect regression. *Holocene*, **15,** 612–618.

Hodell, D.A., Anselmetti, F.S., Ariztegui, D., Brenner, M., Curtis, J.H., Gilli, A., Grzesik, D.A., Guilderson, T.J., Müller, A.D., Bush, M.B., Correa-Metrio, A., Escobar, J. and **Kutterolf, S.** (2008) An 85-ka record of climate change in lowland Central America. *Quatern. Sci. Rev.*, **27,** 1152–1165.

IGME (1982) *Mapa Geológico de España 1:50000 No. 289. Benabarre*. Instituto Geológico y Minero de España, Madrid.

Jopling, A.V. (1975) Early studies on stratified drift. In: *Glaciofluvial and Glaciolacustrine Sedimentation* (Eds A.V. Jopling and B.C. McDonald), *SEPM Spec. Publ.*, **23,** 4–21.

Julià, R. (1980) *La conca lacustre de banyoles*. Centro d'Estudios Comarcals de Banyoles, Besalu, 188 pp.

Kazanci, N., Girgin, S. and **Dügel, M.** (2004) On the limnology of Salda Lake, a large and deep soda lake in southwestern Turkey: future management proposals. *Aquat. Conserv. Mar. Freshwat. Ecosyst.*, **14,** 151–162.

Kelts, K. and **Hsü, K.J.** (1978) Freshwater carbonate sedimentation. In: *Lakes: Chemistry, Geology and Physics* (Ed. A. Lerman), pp. 295–323. Springer-Verlag, New York.

Kindinger, J.L., Davis, J.B. and **Flocks, J.G.** (1999) Geology and evolution of lakes in north-central Florida. *Environ. Geol.*, **38,** 301–321.

Lambiase, J. (1990) A model for tectonic control of lacustrine stratigraphic sequences in continental rift basins. In: *Lacustrine Basin Exploration: Case Studies and Modern Analogues* (Ed. B.J. Katz), *AAPG Mem.*, **50**. 265–276.

Last, W.M. (1990) Paleochemistry and paleohydrology of Ceylon Lake, a salt-dominated playa basin in the northern Great Plains, Canada. *J. Paleolimnol.*, **4,** 219–238.

Last, W.M. and **Vance, R.E.** (1997) Bedding characteristics of Holocene sediments from salt lakes of the northern Great Plains, Western Canada. *J. Paleolimnol.*, **17,** 297–318.

León-Llamazares, A. (1991) *Caracterización agroclimática de la provincia de Huesca*. *Ministerio de Agricultura*, Pesca y Alimentación (M.A.P.A.), Madrid.

López-Vicente, M. (2007) *Erosión y redistribución del suelo en agroecosistemas mediterráneos: Modelización predictiva mediante SIG y validación con 137Cs (Cuenca de Estaña, Pirineo Central)*. Tesis doctoral, Universidad de Zaragoza, Zaragoza, 212 pp.

López-Vicente, M., Navas, A. and **Machín, J.** (2008) Identifying erosive periods by using RUSLE factors in mountain fields of the Central Spanish Pyrenees. *Hydrol. Earth Syst. Sci.*, **12,** 523–535.

Magny, M., de Beaulieu, J.-L., Drescher-Schneider, R., Vannière, B., Walter-Simonnet, A.-V., Millet, L., Bossuet, G. and **Peyron, O.** (2006) Climatic oscillations in central Italy during the Last Glacial-Holocene transition: the record from Lake Accesa. *J. Quatern. Sci.*, **21,** 311–320.

Magny, M., de Beaulieu, J.-L., Drescher-Schneider, R., Vanniere, B., Walter-Simonnet, A.-V., Miras, Y., Millet, L., Bossuet, G., Peyron, O., Brugiapaglia, E. and **Leroux, A.** (2007) Holocene climate changes in the central Mediterranean as recorded by lake-level fluctuations at Lake Accesa (Tuscany, Italy). *Quatern. Sci. Rev.*, **26,** 1736–1758.

Martin, J. (1981) *Le Moyen Atlas centrale: étude géomorphologique*. Editions du Service Géologique, Rabat, Morocco.

Martínez-Peña, M.B. and **Pocoví, A.** (1984) Significado tectónico del peculiar relieve del Sinclinal de Estopiñán (Prepirineo de Huesca). In: *I Congreso Español de Geología, III* (Ed. S.G.D. España), pp. 199–206, Segovia, Spain.

Martín-Puertas, C., Valero-Garcés, B.L., Mata, M.P., González-Sampériz, P., Bao, R., Moreno, A. and **Stefanova, V.** (2008) Arid and humid phases in Southern Spain during the last 4000 years: The Zoñar Lake Record, Córdoba. *Holocene*, **18,** 907–921.

Meyers, P.A. (1997) Organic geochemical proxies of paleoceanographic, paleolimnologic and paleoclimatic processes. *Org. Geochem.*, **97,** 213–250.

Meyers, P.A. and **Lallier-Vergès, E.** (1999) Lacustrine sedimentary organic matter records of Late Quaternary paleoclimates. *J. Paleolimnol.*, **21,** 345–372.

Millet, L., Vannière, B., Verneaux, V., Magny, M., Disnar, J., Laggoun-Défarge, F., Walter-Simonnet, A., Bossuet, G., Ortu, E. and **de Beaulieu, J.-L.** (2007) Response of littoral chironomid communities and organic matter to late glacial lake-level, vegetation and climate changes at Lago dell'-Accesa (Tuscany, Italy). *J. Paleolimnol.*, **38,** 525–539.

Miracle, M.R. and **Gonzalvo, I.** (1979) Els llacs càrstics. *Quaderns d'Ecologia Aplicada* **4,** 37–50.

Mir-Puyuelo, J. (1997) *El Ciclo biogeoquímico del azufre en ecosistemas estratificados. Papel de los compuestos de azufre inorgánico*. Tesis doctoral, Universitat Autonoma de Barcelona, Barcelona.

Mitchum, R.M., Vail, P.R. and **Sangree, J.B.** (1977) Seismic stratigraphy and global changes of sea level, part 6: stratigraphic interpretation of seismic reflection patterns in depositional sequences. In: *Seismic Stratigraphy – Applications to Hydrocarbon Exploration* (Ed. C.E. Payton), *AAPG Mem.*, **26,** 117–133.

Modamio, X., Pérez, V. and **Samarra, F.** (1988) Lirnnologia del lago de Montcortés (ciclo 1978-79) (Pallars Jussá, Lleida). *Oecologia aquatica*, **9,** 9–17.

Morellón, M., Valero-Garces, B., Moreno, A., Gonzalez-Samperiz, P., Mata, P., Romero, O., Maestro, M. and **Navas, A.** (2008) Holocene palaeohydrology and climate variability in Northeastern Spain: the sedimentary record of Lake Estanya (Pre-Pyrenean range). *Quatern. Int.*, **181,** 15–31.

Moreno, A., Valero-Garcés, B., González-Sampériz, P. and **Rico, M.** (2008) Flood response to rainfall variability during the last 2000 years inferred from the Taravilla Lake record (Central Iberian Range, Spain). *J. Paleolimnol.*, **40,** 943–961.

Murphy, D.H. and **Wilkinson, B.H.** (1980) Carbonate deposition and facies distribution in a central Michigan marl lake. *Sedimentology*, **27,** 123–135.

Negendank, J.F.W. and **Zolitschka, B.** (1993) *Paleolimnology of European Maar Lakes*. Springer-Verlag, New York.

Nelson, C.H., Bacon, C.R., Robinson, S.W., Adam, D.P., Bradbury, J.P., Barber, J.H., Schwartz, D. and **Vagenas, G.** (1994) The volcanic, sedimentologic and paleolimnologic history of the Crater Lake caldera floor, Oregon: evidence for small caldera evolution. *Geol. Soc. Am. Bull.*, **106,** 684–704.

Nicod, J. (1999) Phénomènes karstiques et mouvements de terrain récents dans le Dépt. du Var; Risques naturels (Avignon, 1995). pp. 115–130, CTHS, Paris.

Nisbet, E.G. and **Piper, D.J.W.** (1998) Giant submarine landslides. *Nature*, **392,** 329–330.

Olivera, C., Riera, A., Lambert, J., Banda, E. and **Alexandre, P.S.G.d.C.** (1994) *Els terratrèmols de l'any 1373 al Pirineu. Effectes a Espanya i França*. Servei Geològic de Catalunya, Barcelona, 220 pp.

Olivera, C., Redondo, E., Lambert, J., Riera Melis, A. and **Roca, A.** (2006) *Els terratrèmols dels segles XIV i XV a Catalunya*. Barcelona, 407 pp.

Ordóñez, S., Gonzalez Martin, J.A., Garcia del Cura, M.A. and **Pedley, H.M.** (2005) Temperate and semi-arid tufas in the Pleistocene to Recent fluvial barrage system in the Mediterranean area: The Ruidera Lakes Natural Park (Central Spain). *Geomorphology*, **69,** 332–350.

Palmquist, R. (1979) Geologic controls on doline characteristics in mantled karst. *Z. fuer Geomorphol. Suppl Bd*, **32,** 90–106.

Pérez, A., Luzón, A., Roc, A.C., Soria, A.R., Mayayo, M.J. and **Sánchez, J.A.** (2002) Sedimentary facies distribution and genesis of a recent carbonate-rich saline lake: Gallocanta Lake, Iberian Chain, NE Spain. *Sed. Geol.*, **148,** 185–202.

Perez-Obiol, R. and **Julià, R.** (1994) Climatic change on the Iberian Peninsula recorded in a 30 000-yr pollen record from Lake Banyoles. *Quatern. Res.*, **41,** 91–98.

Platt, N.H. and **Wright, V.T.** (1991) Lacustrine carbonates: facies models, facies distribution and hydrocarbon aspects. In: *Lacustrine Facies Analysis* (Eds P. Anadón, L. Cabrera and K. Kelts), *Int. Assoc. Sedimentol. Spec. Publ.*, **13,** 57–74.

Pulido-Bosch, A. (1989) Les gypses triasiques de Fuente Camacho. In: *Réunion franco-espagnole sur les karsts d 'Andalousie*, pp. 65–82.

Ramírez-Moreno, S. (2003) *Técniques de biologia molecular aplicades a l'estudi de sistemes estratificats*. Tesis doctoral, Universitat Autònoma de Barcelona, Bellaterra, Spain, 187 pp.

Reed, J.M. (1998) Diatom preservation in the recent sediment record of Spanish saline lakes: implications for palaeoclimate study. *J. Paleolimnol.*, **19,** 129–137.

Reimer, P.J., Baillie, M.G.L., Bard, E., Bayliss, A., Beck, J.W., Bertrand, C.J.H., Blackwell, P.G., Buck, C.E., Burr, G.S., Cutler, K.B., Damon, P.E., Edwards, R.L., Fairbanks, R.G., Friedrich, M., Guilderson, T.P., Hogg, A.G., Hughen, K.A., Kromer, B., McCormac, G., Manning, S., Ramsey, C.B., Reimer, R.W., Remmele, S., Southon, J.R., Stuiver, M., Talamo, S., Taylor, F.W., van der Plicht, J. and **Weyhenmeyer, C.E.** (2004) IntCal04 terrestrial radiocarbon age calibration, 0–26 Cal Kyr BP. *Radiocarbon*, **46,** 1029–1058.

Renault, R.W. and **Last, W.M.** (1994) *Sedimentology and Geochemistry of Modern and Ancient Saline Lakes*. Society for Sedimentary Geology Special Publication, Tulsa.

Riera, S., Wansard, R. and **Julià, R.** (2004) 2000-year environmental history of a karstic lake in the Mediterranean Pre-Pyrenees: the Estanya lakes (Spain). *Catena*, **55,** 293–324.

Riera, S., Lopez-Saez, J.A. and **Julia, R.** (2006) Lake responses to historical land use changes in northern Spain: the contribution of non-pollen palynomorphs in a multiproxy study. *Rev. Palaeobot. Palynol.*, **141,** 127–137.

Rodó, X., Giralt, S., Burjachs, F., Comín, F.A., Tenorio, R.G. and **Julià, R.** (2002) High-resolution saline lake sediments as enhanced tools for relating proxy paleolake records to recent climatica data series. *Sed. Geol.*, **148,** 203–220.

Romero, L., Camacho, A., Vicente, E. and **Miracle, M.** (2006) Sedimentation patterns of photosynthetic bacteria based on pigment markers in Meromictic Lake La Cruz (Spain): paleolimnological implications. *J. Paleolimnol.*, **35,** 167–177.

Romero-Viana, L., Julià, R., Camacho, A., Vicente, E. and **Miracle, M.** (2008) Climate signal in varve thickness: Lake La Cruz (Spain), a case study. *J. Paleolimnol.* **40,** 703–714.

Sadori, L. and **Narcisi, B.** (2001) The Postglacial record of environmental history from Lago di Pergusa, Sicily. *Holocene*, **11,** 655–671.

Sancho-Marcén, C. (1988) El Polje de Saganta (Sierras Exteriores pirenaicas, prov. de Huesca). *Cuaternario y Geomorfología*, **2,** 107–113.

Schilts, W.W. and **Clague, J.J.** (1992) Documentation of earthquake-induced disturbance of lake sediments using subbottom acoustic profiling. *Can. J. Earth Sci.*, **29,** 1018–1042.

Schmidt, R., Müller, J., Drescher-Schneider, R., Krisai, R., Szeroczynska, K. and **Baric, A.** (2000) Changes in lake level and trophy at Lake Vrana, a large karstic lake on the Island of Cres (Croatia), with respect to palaeoclimate and anthropogenic impacts during the last approx. 16 000 years. *J. Limnol.*, **59,** 113–130.

Schnellmann, M., Anselmetti, F.S., Giardini, D. and **McKenzie, J.A.** (2005) Mass movement-induced fold-and-thrust belt structures in unconsolidated sediments in Lake Lucerne (Switzerland). *Sedimentology*, **52,** 271–289.

Schnurrenberger, D., Russell, J. and **Kelts, K.** (2003) Classification of lacustrine sediments based on sedimentary components. *J. Paleolimnol.*, **29,** 141–154.

Schreiber, B.C. and **Tabakh, M.E.** (2000) Deposition and early alteration of evaporites. *Sedimentology*, **47,** 215–238.

Shaw, B., Klessig, L. and **Mechenich, C.** (2002) *Understanding Lake Data*. University of Wisconsin Cooperative Extension, Madison.

Smoot, J.P. and **Lowenstein, T.** (1991) Depositional environments of non-marine evaporites. In: *Evaporites, Petroleum and Mineral Resources* (Ed. J. Melvin), *Dev. Sedimentol.*, **50,** 189–348. Elsevier, Amsterdam.

Strasser, M., Stegmann, S., Bussmann, F., Anselmetti, F.S., Rick, B. and **Kopf, A.** (2007) Quantifying subaqueous slope stability during seismic shaking: Lake Lucerne as model for ocean margins. *Mar. Geol.*, **240,** 77–97.

Street-Perrott, F.A. and **Harrison, S.P.** (1985) Lake levels and climate reconstruction. In: *Paleoclimate Analysis and Modeling* (Ed. A. Hecht), pp. 291–340. Wiley, New York.

Talbot, M.R. and **Allen, P.A.** (1996) Lakes. In: *Sedimentary Environments: Processes, Facies and Stratigraphy* (Ed. H.G. Reading), pp. 83–124. Blackwell Science, Oxford.

Valero Garces, B.L., Moreno, A., Navas, A., Mata, P., Machin, J., Delgado Huertas, A., Gonzalez Samperiz, P., Schwalb, A., Morellon, M., Cheng, H. and **Edwards, R.L.** (2008) The Taravilla lake and tufa deposits (Central Iberian Range, Spain) as palaeohydrological and palaeoclimatic indicators. *Palaeogeogr. Palaeoclimatol. Palaeoecol.*, **259,** 136–156.

Valero-Garcés, B.L. and **Kelts, K.R.** (1995) A sedimentary facies model for perennial and meromictic saline lakes: Holocene Medicine Lake Basin, South Dakota, USA. *J. Paleolimnol.*, **14,** 123–149.

Valero-Garcés, B., Navas, A., Machín, J., Stevenson, T. and **Davis, B.** (2000) Responses of a saline Lake Ecosystem in a semiarid region to irrigation and climate variability: the history of Salada Chiprana, Central Ebro Basin, Spain. *Ambio*, **29,** 344–350.

Valero-Garcés, B., Navas, A., Mata, P., Delgado-Huertas, A., Machín, J., González-Sampériz, P., Moreno, A., Schwalb, A., Ariztegui, D., Schnellmann, M., Bao, R. and **González-Barrios, A.** (2003) Sedimentary facies analyses in lacustrine cores: from initial core descriptions to detailed palaeoenvironmental reconstructions. A case study from Zoñar Lake (Cordoba province, Spain). In: *Limnogeology in Spain: A Tribute to Kerry Kelts* (Ed. B. Valero-Garcés), *Bibl. Cienc.*, **14,** 385–414. C.S.I.C., Madrid.

Valero-Garcés, B., González-Sampériz, P., Navas, A., Machín, J., Delgado-Huertas, A., Peña-Monné, J.L., Sancho-Marcén, C., Stevenson, T. and **Davis, B.** (2004) Palaeohydrological fluctuations and steppe vegetation during the Last Glacial Maximum in the central Ebro valley (NE Spain). *Quatern. Int.*, **122,** 43–55.

Valero-Garcés, B., González-Sampériz, P., Navas, A., Machín, J., Mata, P., Delgado-Huertas, A., Bao, R., Moreno, A., Carrión, J.S., Schwalb, A. and **González-Barrios, A.** (2006) Human impact since medieval times and recent ecological restoration in a Mediterranean lake: the Laguna Zoñar, southern Spain. *J. Paleolimnol.*, **35,** 441–465.

Villa, I. and **Gracia, M.L.** (2004). *Estudio hidrogeológico del sinclinal de Estopiñán (Huesca)*. XXXVIII CHIS. Confederación Hidrográfica del Ebro, Zaragoza.

Wansard, G., De Deckker, P. and **Julia, R.** (1998) Variability in ostracod partition coefficients D(Sr) and D(Mg): implications for lacustrine palaeoenvironmental reconstructions. *Chem. Geol.*, **146,** 39–54.

Wright, V.P. (1990) Lacustrine carbonates. In: *Carbonate Sedimentology* (Ed. M.E. Tucker and V.P. Wright), pp. 164–190. Blackwell Scientific Publications, Oxford.

Zanchetta, G., Borghini, A., Fallick, A., Bonadonna, F. and **Leone, G.** (2007) Late Quaternary palaeohydrology of Lake Pergusa (Sicily, southern Italy) as inferred by stable isotopes of lacustrine carbonates. *J. Paleolimnol.*, **38,** 227–239.

Manuscript received 11 April 2008; revision accepted 13 November 2008